RESPONSE OF AN IDEALIZED ROTATING BLADE WITH A NONLINEAR ELASTOMER

By

Narmadeshwar Jha

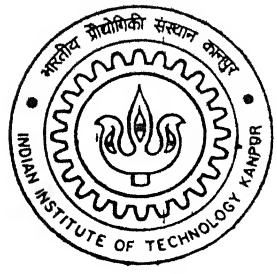

DEPARTMENT OF MECHANICAL ENGINEERING

Indian Institute of Technology Kanpur

JANUARY, 2002

RESPONSE OF AN IDEALIZED ROTATING BLADE WITH A NONLINEAR ELASTOMER

A Thesis Submitted
in Partial Fulfillment of the Requirements
for the Degree of
MASTER OF TECHNOLOGY

by

Narmadeshwar Jha

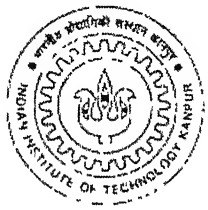

to the

DEPARTMENT OF MECHANICAL ENGINEERING
INDIAN INSTITUTE OF TECHNOLOGY KANPUR

January, 2002

CERTIFICATE

It is certified that the work contained in the thesis entitled "***Response of an Idealized Rotating Blade With a Nonlinear Elastomer***" by Narmadeshwar Jha (Roll No. Y010532) has been carried out under our supervision and this work has not been submitted elsewhere for a degree.

Dr. A. K. Mallik

Department of Mechanical Engineering

Indian Institute of Technology, Kanpur

Dr. C. Venkatesan

Department of Aerospace Engineering

Indian Institute of Technology, Kanpur

January 4, 2002

ACKNOWLEDGEMENT

I wish to express my profound gratitude and indebtedness towards my thesis supervisors Dr. A.K. Mallik and Dr. C. Venkatesan for their inspiring guidance, invaluable suggestions and constant encouragement. Their openness and grant of adequate freedom to me for thesis work, kept my thought process unbridled.

I am extremely thankful to Ajeet, Arvind, Durgesh, Kuldeep, Lalit, Lt. M. V Rao, Onkar, Pankaj, Saurabh, and Subodh, who devoted their valuable time and helped me in all possible ways towards successful completion of my thesis work. I appreciate and extend my thanks to all those who have contributed directly or indirectly to my thesis.

I would like to thank all my friends for making my stay at IITK very enjoyable and memorable. I will cherish the moments forever.

Finally, I am grateful to the Almighty, my parents, Bhaiya and all other family members for what I am today.

Indian Institute of Technology, Kanpur. *Narmadeshwar Jha*

January 4, 2002

ABSTRACT

The dynamic characteristics of the rotor blade play a significant role in the overall performance and stability of the vehicle. In general, the elastomer used in a bearingless rotor exhibits highly non-linear characteristics both in stiffness and damping with respect to the amplitude of deformation. It is expected that due to the presence of the elastomer, the lag and flap frequencies should dependent on the amplitude of motion, which is a typical feature of a non-linear system. The transient response analysis of a bearingless rotor blade requires the formulation of equations of motion representing coupled axial, flap-lag, and torsional motion of the blade. In the present work, a preliminary study has been carried out considering two elastomeric models. The effect of flap-lag coupling is investigated towards the occurrence of limit cycle oscillations. It is observed that there is no limit cycle oscillation when there is no coupling between the lag and flap modes. Also the coupling is of one –way type i.e., there is no energy transfer from lag mode to flap mode but the reverse is not true. The data used in the preliminary study to formulate the elastomer damper model is based on lag damper bench tests conducted at single frequency excitation. Since the lead lag motion occurs at multiple frequencies simultaneously, the damper properties may not be adequately predicted by a linear superposition of the damper properties at each of the motion frequencies. In this work, the dual frequency analysis has been carried out and the damper models are characterized in terms of in-phase stiffness and quadrature stiffness.

CONTENTS

LIST OF FIGURES

Fig. No. *Description* *Page No.*

LIST OF SYMBOLS

K_1, K_3, K_5, K_7	stiffness parameters of non-linear spring
X	amplitude of motion
K'	in-phase stiffness of elastomer damper model
K''	quadrature stiffness of elastomer damper model
h	hysteretic damping coefficient of elastomermodel 1
h_1, h_3	hysteretic damping coefficients of elastomer model 2
ω	frequency
Ω	angular speed of rotor
F	coulomb damping force
ξ	displacement in lag direction
β	displacement in flap direction
F_c, F_s	cosine and sine component of force
X_c, X_s	cosine and sine component of displacement
t	time
V	velocity
T	kinetic energy
U	potential energy
Q_{nc}	non-conservative moment associated with lag mode
$Q_{nc\beta}$	non-conservative moment associated with flap mode
l	length of helicopter rotor blade
m	mass per unit length of helicopter rotor blade
e	hinge offset
τ	non-dimensional time
F_1, F_2	exciting forces at ω_1 and ω_2

LIST OF TABLES

CHAPTER-1
INTRODUCTION

1.1. INTRODUCTION

The main rotor system of a helicopter is the most important component of the vehicle. The dynamic characteristics of rotor blade play a significant role in the overall performance and stability of the vehicle. There has been a continued effort to develop a mechanically simple and efficient rotor blade and hub configuration. With the advancement in technology, development of a mechanically simple yet efficient rotor blade system has resulted in the design of a bearingless rotor blade and hub configuration. In the bearingless rotor blade and hub configuration an elastomeric damper is placed to provide adequate lag damping. Elstomer materials are becoming increasingly popular for vibration attenuation application due to the tremendous advantages they offer over mechanical dampers. It is well known that under dynamic conditions, elastomeric materials exhibit visco-elastic behavior dissipating energy through hysteresis.

1.2. EARLY ROTOR SYSTEMS: A REVIEW

In order to relieve the root bending moments experienced by the blades, early rotor blades were provided with flap (out of plane bending) and lag (in-plane bending) hinges at the root of the blade. In addition, a pitch control bearing was provided to

control the pitch angle of the blade. Such rotor systems are usually referred to as articulated rotors. While the provision of the hinges represent an efficient engineering solution to the problem of alleviating high bending loads at the root, there are several disadvantages of this type. The large number of moving parts leads to a mechanically complex rotor hub system, accompanied by the associated wear out problem requiring frequent maintenance and replacement of parts. The presence of hinges prevents generation of large control moments.

With the advancement in fibre-reinforced composite material technology, increasing emphasis has been placed on the development of hingeless rotor systems. The construction of these rotors is relatively simple because of the absence of flap and lag hinges; but a pitch bearing is still provided for blade pitch control. Due to the absence of hinges, large control moments can be generated which in turn provide favorable control characteristics of the vehicle. Both articulated and hingeless rotors are provided with external hydraulic dampers to increase damping in the lag mode and thereby to avoid aeroelastic and aeromechanical instabilities.

1.3 GENERAL PROPERTIES OF ELASTOMERS

Under dynamic condition elastomeric materials exhibit visco-elastic behavior dissipating energy through hysteresis. Due to the visco-elastic nature of the material, damping and stiffness properties of the elastomers are complex functions of the displacement, amplitude, frequency and even temperature.

A typical static load deflection curve for a non-linear visco-elastic material is shown in Figure (1.1) by the curve OABC. Generally the static nonlinear characteristics of the elastomers are described by the secant stiffness evaluated at different values of the deflection. For example, the slopes of the line OA and OB define the secant stiffness at points A and B, respectively.

The load deflection curve of the elastomer under dynamic loading about these two equilibrium points A and B can be represented by the corresponding visco-elastic hysteresis loops superimposed on the equilibrium curve OABC at the points A and B, respectively. The dynamic stiffness values at A and B are defined

by the slopes of the line pq and $p'q'$, where the points p, q, p' and q' are the points corresponding to the maximum deflection of the elastomer as shown in Fig (1.1). On the other hand, linearised stiffness is defined using static load – deflection curve. The slopes of the lines uv and $u'v'$ represent the linearised stiffness values in the vicinity of the equilibrium points A and B respectively.

The stiffness modulus is defined as the in-phase force component that is required to produce unit amplitude of harmonic deformation. Similarly the damping modulus is defined as the required force component (for unit amplitude of deformation) that is in quadrature with the deformation. The dynamic stiffness and damping values can also be identified from the hysteresis cycles for different amplitudes of motion. The area of the hysteresis loop provides the information about the amount of energy dissipated per cycle at particular amplitude of deformation. Typical hysteresis cycle of a non-linear elastomeric material about non-zero equilibrium position is shown in Fig. (1.2). It can be observed from Fig. (1.2) that when the amplitude of motion is X_1, the slope of the line a_1b_1 gives the corresponding dynamic stiffness. When the amplitude of motion is increased to X_2 the slope of the line a_2b_2 represents the dynamic stiffness. It is evident that these two stiffness values can be different depending upon the distortion of the hysteresis loop with the amplitude of motion. However the linearised stiffness about the zero equilibrium point is given by the slope of the static load deflection curve $a_2a_1ob_1b_2$ at o i.e. slope of the line lm. It is important to note that the linearised stiffness can be different from the dynamic stiffness for a given amplitude. Also the dynamic stiffness is a function of the amplitude of motion. Therefore, in any linearised stability analysis, the effect of the change in the stiffness due to change in the amplitude of motion is not at all taken into account.

The area of the corresponding hysteresis loop gives the energy dissipated by the visco-elastic material for the particular amplitude of motion. Figure (1.2) also indicates that the energy dissipated per cycle depends on the amplitude of motion.

1.4 THE ELASTOMERIC DAMPERS

Many helicopters use elastomeric lag dampers to prevent ground resonance and aeroelastic instability in hover and forward flight. With the development of simple and efficient rotor systems, elastomeric materials are being widely used in replacing the conventional bearing and hydraulic dampers in helicopter rotor systems. Elastomeric bearings are replacing thrust bearings in transferring large centrifugal load at the blade root.

ADVANTAGE OF ELASTOMERIC DAMPERS: -

1. The elastomeric dampers are simpler.
2. They have no moving parts.
3. They do not require mechanical seals and lubricants.
4. They do not produce extremely high damping forces at high lead –lag velocities that characterize hydraulic dampers.

As a result of these advantages, the trend in new helicopter design is clearly away from hydraulic dampers and towards elastomeric dampers.

Unlike hydraulic dampers, the elastomeric dampers have stiffness. But the stiffness and damping characteristics of these dampers are non-linear function of the frequency and amplitude of the blade lag motion.

1.5 BEARINGLESS ROTOR SYSTEM WITH ELASTOMERIC DAMPERS

The development of bearingless rotor systems aims to eliminate both the pitch bearing as well as the external damper by incorporating a specialized elastomer with high loss factor. Elastomeric material characteristics (stiffness and damping or elastic modulus and loss factor) are highly non-linear and are dependent on operating temperature, frequency, amplitude of motion and mean stress level. Elastomeric damper seems to have a significant influence on the limit cycle oscillation of the rotor blade.

Figure (1.3) shows a typical bearingless rotor system. In this rotor system, the blade is attached to the hub through a flexible structural element called flexbeam The flexbeam is designed to provide the required stiffness in the flap and lag bending deformations of the blade, but it is highly flexible in torsion. The pitch control of the blade is achieved by rotating the torque tube through up and down movement of the point P, which in turn twists the flexbeam. An elastomer is placed between the torque tube and the flexbeam to provide adequate lag damping. Though the bearingless rotor is mechanically simple, its dynamic analysis becomes very complicated due to presence of multiple load paths, non-linear elastomeric dampers and existence of kinematic constraint at the pitch link.

For the analysis and design of the bearingless rotor blades, most of the rotorcraft manufacturers have developed their own in-house methodologies and computer codes. Hence, very little information is available about them in open literature.

1.6 LITERATURE REVIEW

Due to the presence of elastomeric dampers in bearingless rotors, it is essential to characterize the non-linear behavior of the elastomer and to develop a suitable model, which can be easily integrated in the structural dynamics and aeroelastic analysis of the rotor blades. There are several linear models used to describe the mechanical behavior of visco-elastic materials. The non-linear characteristics of elastomers have been analyzed in detail in several recent publications. Some of the recent studies have focused on the phenomenon of limit cycle behavior of bearingless rotor blades due to elastomer non-linearity. Elastomeric material characteristics (stiffness and damping or elastic modulus and loss factor) are highly non-linear and are dependent on operating temperature, frequency, amplitude of motion and mean stress level. It has been a very challenging task to develop an analytical model that can accurately represent the behavior of the elastomeric dampers.

For visco-elastic materials, the stress-strain relation depends on the time history. Classical linear constitutive relations for visco-elastic materials are formulated either in the time domain or in the frequency domain [1]. Many theories have been proposed to model the non-linear behavior of visco-elastic materials using hereditary integral representation. Glockner and Szyszkowski [2,3] proposed a semi empirical constitutive model to predict creep, strain softening and relaxation behavior. These non-linear models, being in the integral form, cannot be conveniently incorporated into the structural dynamics analysis.

A review on the performance of elastomeric devices can be found in Ref. [4]. McGuire [5] conducted experiments at Lord Corporation to identify the non-linear behavior of an elastomer. Experiments carried out by Housmann [6,7] indicated that most of the elastomeric materials show significant non-linear behavior so far as the frequency and amplitude of motion are concerned. He also proposed a thermo-mechanical model to include the temperature effects. Felker et al. [8] carried out experiments to determine the properties of an elastomeric lag damper used in Bell model 412 Helicopter. A non-linear model was proposed in which both the stiffness and damping characteristics were expressed as function of displacement. Later on Gandhi and Chopra [9] proposed an elastomeric damper model to simulate a reduction in damping at very low dynamic amplitudes. With this elastomeric damper model, they showed a limit cycle oscillation for an autonomous system representing isolated lag dynamics of a blade. Ormiston et al. [10] proposed a combination of a non-linear spring and a Kelvin chain with nonlinear damping and spring elements. The damping element was represented by a linear combination of terms having fraction, linear, quadratic, and cubic powers of velocity.

It has been observed experimentally that neither the linear nor the non-linear model is capable of accurately predicting the response of the blade under a large impulsive loading. Of course, the non-linear model performed better than the linear one [11]. Hence one can conclude that all elastomeric models have certain limitations for application to the analysis of transient response, steady state response and stability of rotor blades.

Pohit [13] formulated a simple non-linear model to represent the non-linear stiffness and damping characteristics of an elastomer and studied its influence on the isolated lag and flap dynamics of a rotor blade.

For lead lag motion that occur at multiple frequencies simultaneously, the damper properties may not be adequately predicted by a linear superposition of the damper properties at each of the motion frequencies. Felker et al [8] presented the result of elastomeric bench tests. They also investigated the behavior of an elastomeric lag damper undergoing dual frequency motion and its effect on rotor system dynamics.

1.7 EXPERIMENTAL DATA OF ELASTOMERIC DAMPERS

The experimental results of single frequency bench test of different elastomeric lag dampers have been given in Refs. 7, 8, 11 and 12. The mathematical relation between exciting force and displacement is generally represented as

$$F = F_0 e^{i\omega t} = \left(K' + iK''\right) X_0 e^{i\omega t}$$

Where F, ω, and X_0 represent the excitation force, the frequency of excitation and the amplitude of displacement, respectively. The symbols K' and K'' are used to represent the stiffness of elastomer and defined as in-phase stiffness and the quadrature stiffness, respectively. The loss tangent or tangent loss factor (η) is defined as the ratio of K'' over K'. It is important to recognize that K' and K'' are functions of amplitude of motion (X_0), frequency (ω) and temperature.

The experimental data of single frequency and dual frequency bench tests of an elastomeric damper are given in Ref.[8]. For single frequency excitation, the data corresponding to in-phase stiffness and quadrature stiffness with respect to amplitude of motion are shown in Figure 1.4.

Initially both K' and K'' decrease drastically as the amplitude of motion is increased and subsequently both reach asymptotic values at high amplitude of motion. In the frequency range of excitation, i.e., 3.3 Hz to 6.8 Hz, both K' and K'' seem to be independent of the frequency of excitation. Experimental data given in Refs. 7, 11 and 12 follow similar trend, as shown in Figure 1.4.

The experimental data corresponding to dual frequency excitation are shown in Figure 1.5 (taken from Ref.[8]). In this case, the elastomeric damper was excited by a signal which is a linear combination of two frequencies namely 3.3 Hz and 5.4 Hz, having different amplitude of motion. Performing a Fourier analysis of the output signal, the stiffness quantities corresponding to two input frequencies are obtained. The in-phase and quadrature stiffness values, corresponding to the harmonic frequency 5.4 Hz, are plotted as a function of amplitude of motion. Each curve in Figure 1.5 corresponds to different amplitude of the component having frequency 3.3 Hz. It is observed that inclusion of additional input at frequency 3.3 Hz, decreases the value of both in-phase and quadrature stiffness at low amplitude of motion.

1.8 OBJECTIVE OF THE PRESENT STUDY

The general conclusion of the literature survey is that all elastomeric models have certain limitations for applications to the analyses of the transient response and stability of rotor blades. It was observed that neither the linear nor the non-linear model was capable of accurately predicting the response of the blade. Of course, the non-linear model performed better than the linear one. It was also observed that the elastomer used in a bearingless rotor shows highly non-linear characteristics both in stiffness and damping with respect to the amplitude of deformation. Therefore it is expected that due to the presence of elastomer, the lag and flap frequencies should be dependent on the amplitude of motion.

Pohit et al. [13,14,15 and 16] carried out modeling of elastomeric lag dampers. He used the experimental data as given in Ref. [8] [shown in Figure (1.4)] and proposed two mathematical models representing the same set of data. Since the static stress-strain curve of an elastomeric material is non-linear, it is logical to assume the restoring element to be non-linear. The restoring force for both models is assumed to be of seventh order and the values of different constants were found out using error minimization technique. The experimental data [Figure (1.4)] do not exhibit any significant dependence on frequency within the range of interest

(3.3 Hz to 6.8 Hz). Therefore the damping was represented by a combination of Coulomb damper and a hysteretic damper. The reason for choosing Coulomb damper is that the damping force is very high at low amplitude; in addition both coulomb and hysteretic dampers provide damping forces, which are independent of frequency.

1) In Model 1 the elastomer is modeled as a parallel combination of a nonlinear spring, a coulomb damper and a hysteretic damping element.
2) The second model consists of a non-linear spring, a coulomb damping element, and a Rayleigh type hysteretic damping element.

Hysteretic damping in case of Model 1 is assumed as linear while of Model 2 it is of third order. Using these two models Pohit carried out a study on the aeroelastic response of helicopter rotors. Using the Model 1 and Model 2, the transient response characteristics of the helicopter rotor blade to a step input in pitch angle, was obtained. In the case of Model 2 (Figure 1.6), it was observed that within a short time, the lag response settles down to a stable limit cycle oscillation. In the case of Model 1(Figure 1.7), the transient response in lag mode settles to steady state. In other words, the response of Model 2 exhibits a limit cycle oscillation whereas no such oscillation is observed for Model 1, although both models represent same set of data points.

The study carried out by Pohit [13] included several complex factors simultaneously. Therefore, no particular factor can be said to be responsible for aeroelastic instability. The aim of the present study is to find out the cause of occurrence of limit cycle oscillation and the reason for the different responses shown by Model 1 and Model 2, even though they represent the same set of data points. In the present study, the analysis has been carried out for various dynamical systems of increasing complexity to identify the influence of modeling of elastomers on the system response. Hence, the objectives of the present study are:

1. To study the elastomer damper model in non-rotating mode of motion;

2. To study the response of the model in uncoupled lead lag motion of the rotor blade;
3. Examine the response of the model in the coupled flap-lag motion of rotor blade and investigate for the occurrence of limit cycle oscillation, and
4. Examine the elastomeric damper model under dual frequency excitation.

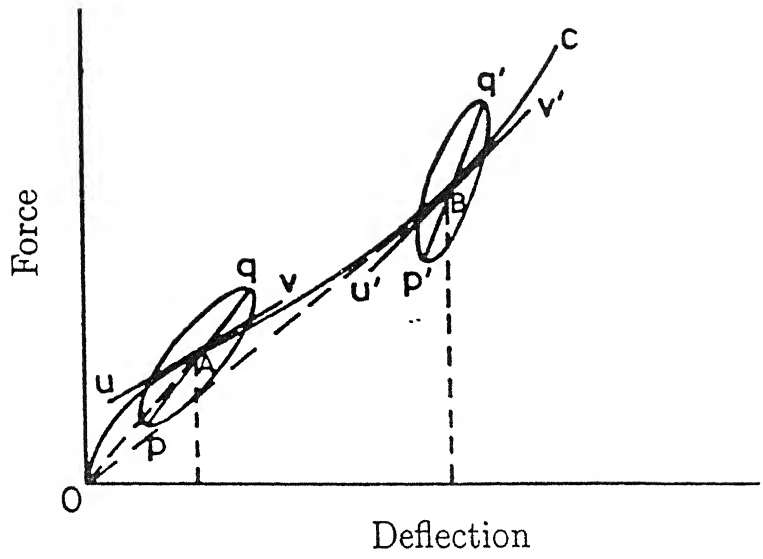

Figure 1.1 Non-linear Dynamic Characteristic of a Visco-elastic Material

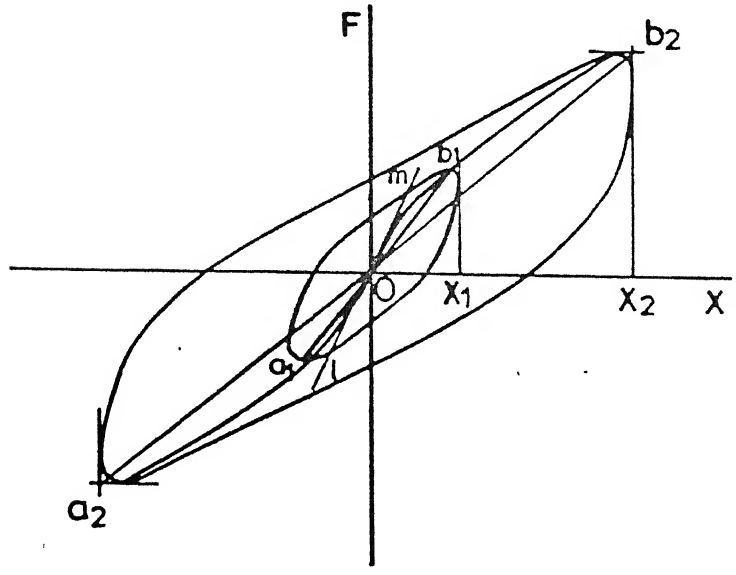

Figure 1.2 Hysteresis cycles of a Non-linear material about zero equilibrium point

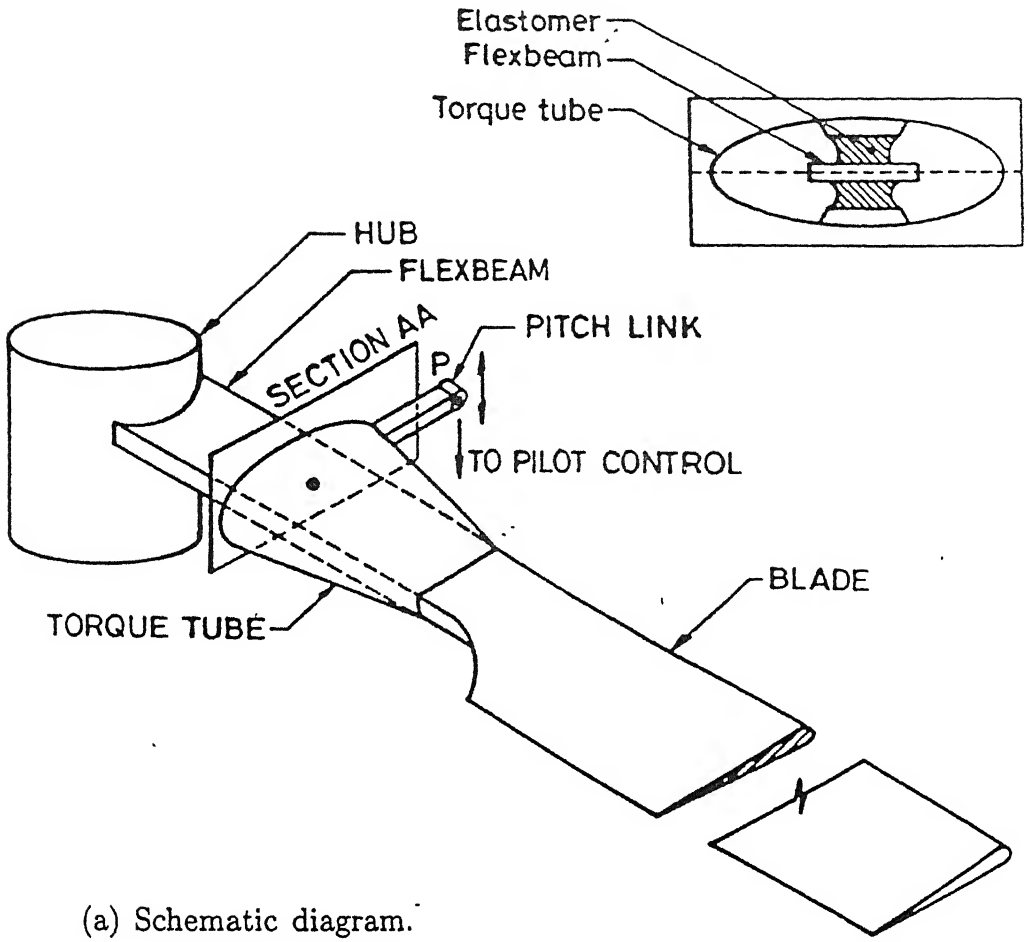

(a) Schematic diagram.

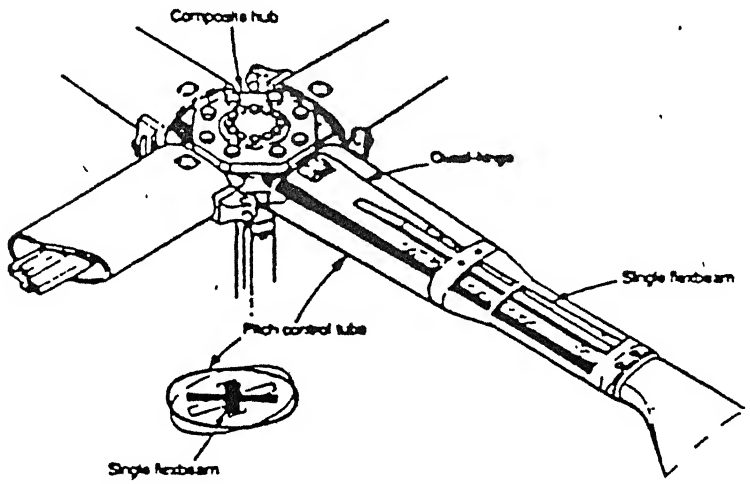

Figure 1.3 Bearingless Rotor Hub and Blade Configuration.

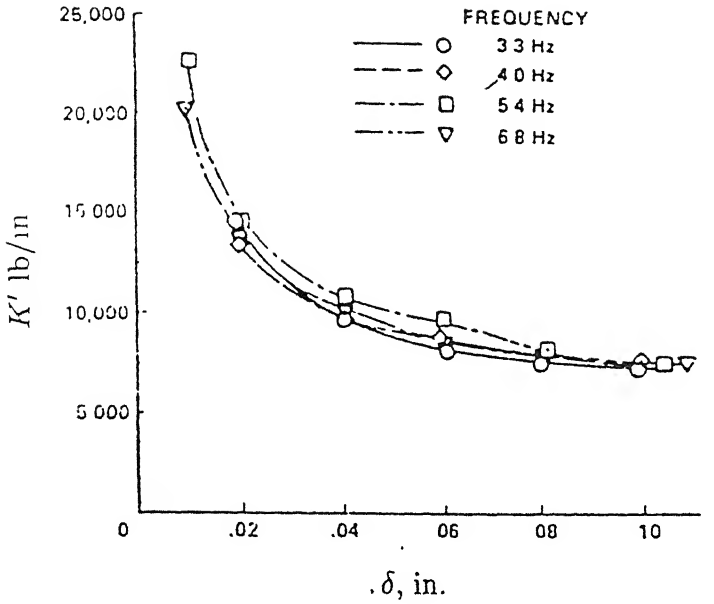

(a) In-phase stiffness

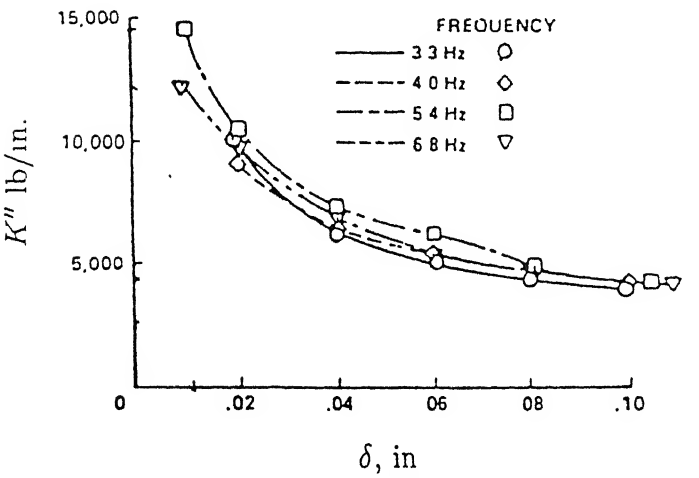

(b) Quadrature stiffness

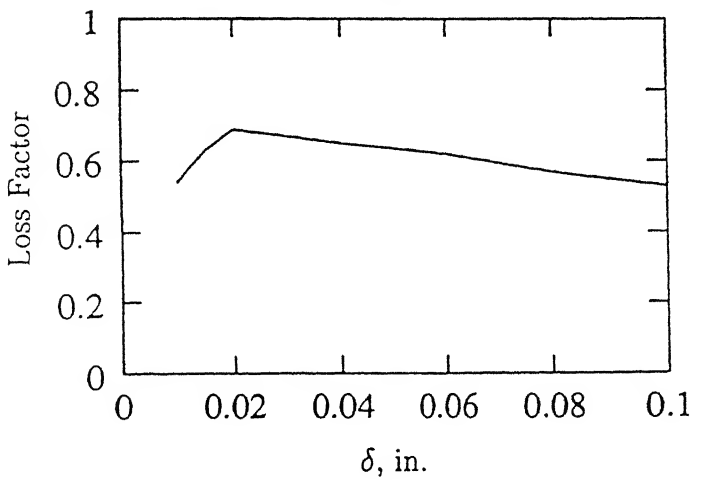

(c) Loss factor (computed)

Figure 1.4 Variation of complex moduli with amplitude for single frequency excitation

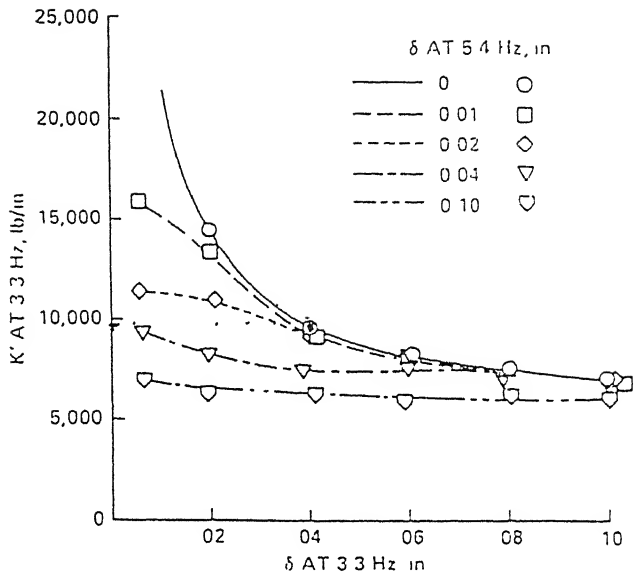

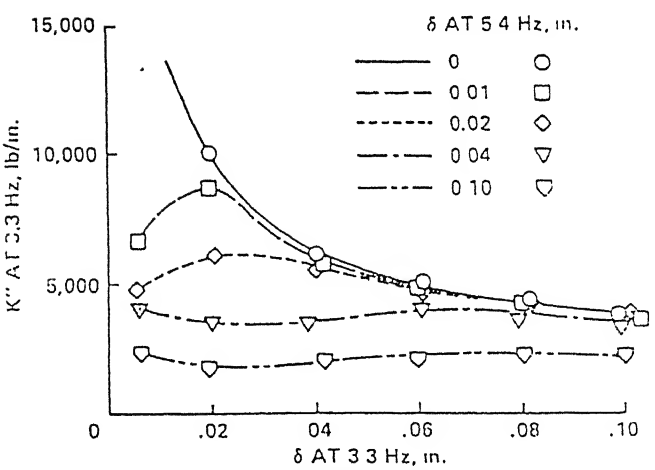

Figure 1.5a Variation of complex moduli with amplitude for dual frequency excitation

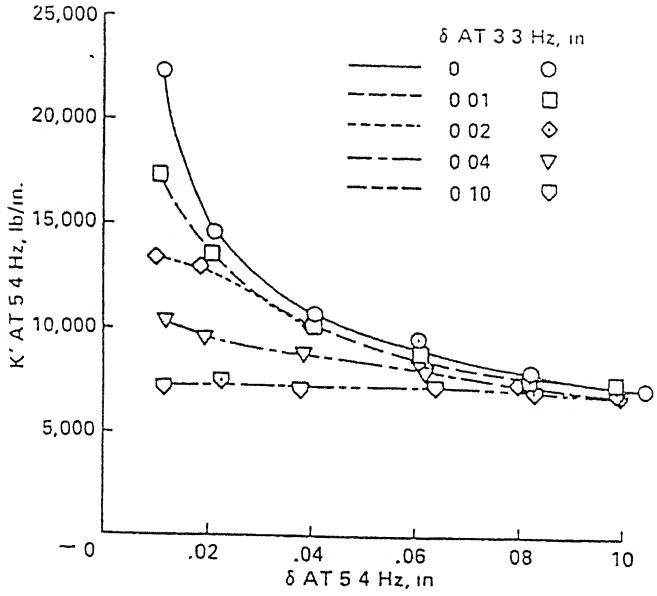

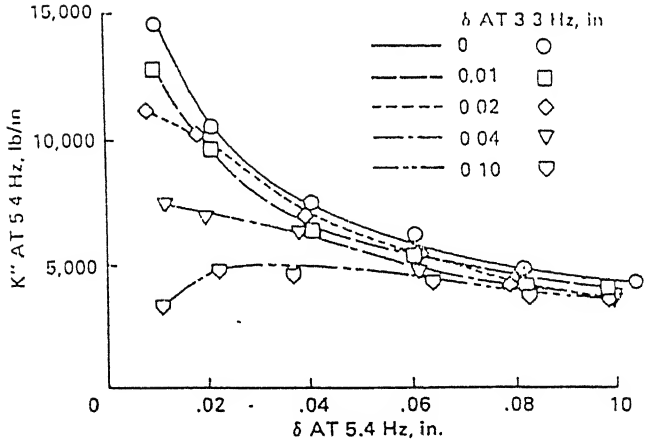

Figure 1.5b Variation of complex moduli with amplitude for dual frequency excitation

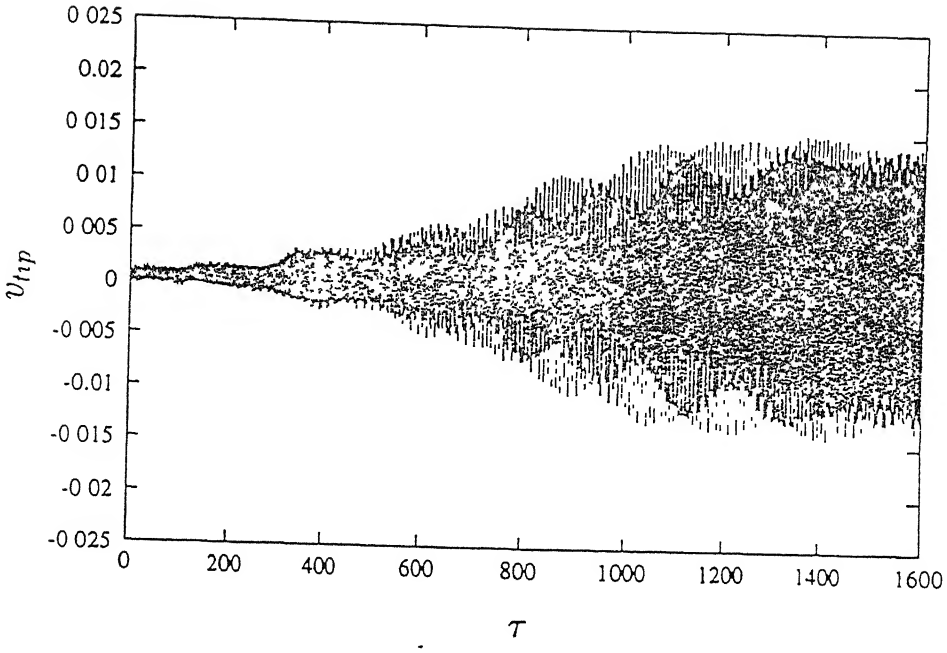

Figure 1.6 Transient response in lag mode with Model 2

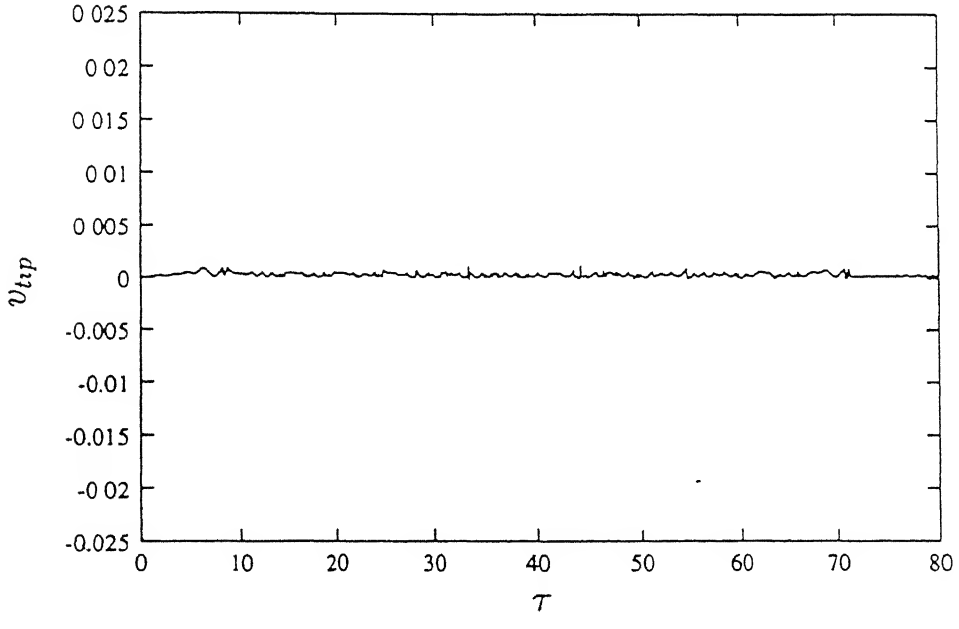

Figure 1.7 Transient response in lag mode with Model 1

CHAPTER-2

RESPONSE OF A NON-ROTATING SYSTEM WITH ELASTOMER

2.1. INTRODUCTION

Pohit [16] investigated the response of elastomeric damper model and showed that Model 2 exhibits a limit cycle oscillation whereas no such oscillation is observed for Model 1, although both models represent same set of data points. To find out the possible causes of this behavior of elastomer damper model it is essential to carry out the study in a very systematic way starting from a very simple case and then adding other factors one-by-one to increase the complexity. In the present chapter, analysis has been carried out for a very simple case where elastomer damper is attached to a non-rotating mass, as shown in Fig. 2.3.

2.2. ELASTOMERIC DAMPER MODELS

Two models proposed by Pohit (Figure 2.1) correspond to: -

1) Model 1: - the elastomer is modeled as a parallel combination of a nonlinear spring, a coulomb damper and a hysteretic damping element.
2) Model 2: - model 2 consists of a non-linear spring, a coulomb damping element, and a Rayleigh type hysteretic damping element.

2.2.1 *MODEL-1*

The constitutive differential equation of motion with elastomer Model 1 under harmonic loading is given by

$$K_1 x - K_3 x^3 + K_5 x^5 - K_7 x^7 + F \operatorname{sgn} | \dot{x} | + \frac{h}{\omega} \dot{x} = D_0 \sin \omega t \ldots\ldots\ldots (2.1)$$

The non-linear dynamic characteristics of the elastomer are usually represented by the variation of in-phase stiffness (stiffness) and the quadrature stiffness as a function of amplitude. The in-phase stiffness K' and the quadrature stiffness K'' for model (1) can be obtained as

$$K' = K_1 - \frac{3}{4} K_3 X^2 + \frac{5}{8} K_5 X^4 - \frac{1}{2} K_7 X^6 \ldots\ldots\ldots\ldots\ldots\ldots (2.2)$$

$$K'' = \frac{4F}{\pi X} + h \ldots\ldots\ldots\ldots\ldots\ldots\ldots\ldots\ldots\ldots\ldots\ldots\ldots\ldots\ldots\ldots (2.3)$$

Where D_0 is the amplitude of exciting force and K_1, K_3, K_5, K_7, F, and h are system parameters of the elastomer and X is the amplitude of motion.

2.2.2 *MODEL-2*

The differential equation of motion with elastomer Model (2) is given by

$$K_1 x - K_3 x^3 + K_5 x^5 - K_7 x^7 + F \operatorname{sgn} | \dot{x} | - \frac{h_1}{\omega} \dot{x} + \frac{h_3}{\omega^3} \dot{x}^3 = D_0 \sin \omega t. (2.4)$$

The in-phase stiffness K' and the quadrature stiffness K'' for model (2) can be obtained as

$$K' = K_1 - \frac{3}{4} K_3 X^2 + \frac{5}{8} K_5 X^4 - \frac{1}{2} K_7 X^6 \ldots\ldots\ldots\ldots\ldots\ldots (2.5)$$

$$K'' = \frac{4F}{\pi X} + \frac{3}{4} h_3 - h_1 \ldots\ldots\ldots\ldots\ldots\ldots\ldots\ldots\ldots\ldots\ldots\ldots\ldots\ldots\ldots\ldots (2.6)$$

In this case one can see that the term corresponding to Rayleigh type hysteretic damping changes sign with varying amplitudes.

The system parameters for both the models are tabulated in Table 2.1 and the correlation of both with experimental data is shown in Fig. 2.2.

2.3 ELASTOMERIC DAMPER MODELS WITH MASS

The idealized elastomeric damper model attached with a non-rotating mass is shown in Figure (2.3). The equation of motion for a system with Model 1 and a lumped mass m undergoing free vibration can be written as

$$m\ddot{x}+K_1x-K_3x^3+K_5x^5-K_7x^7+F\,\mathrm{sgn}\,|\dot{x}|+\frac{h}{\omega}\dot{x}=0.....(2.7)$$

And for a system with model-2 the equation of motion in free vibration can be written as

$$m\ddot{x}+K_1x-K_3x^3+K_5x^5-K_7x^7+F\,\mathrm{sgn}\,|\dot{x}|-\frac{h_1}{\omega}\dot{x}+\frac{h_3}{\omega^3}\dot{x}^3=0.....(2.8)$$

These equations are non –linear differential equations. In most of the non-linear dynamics problems, an exact solution is not possible. Researchers generally follow the method of numerical techniques. Here, solutions are obtained by *Fourth Order Runge-Kutta* method. The response of the system was obtained for various combinations of initial conditions.

2.4 RESULTS AND DISCUSSION

The responses of elastomer damper Model 1 and Model 2 in non-rotating mode are shown in Fig. 2.4(a) and Fig. 2.4(b) for initial disturbance 0.002m. Figure 2.5(a) and Fig. 2.5(b) are the responses of the system for Model 1 and Model 2, respectively when initial disturbance is 0.003m. In these calculations, the mass attached (6214.73 Kg) is so chosen that it corresponds to the natural frequency of the system as 3.3 Hz taking linear stiffness term only. The results showed that both proposed models exhibit almost same results for the non-rotating when initial disturbance is 0.002m and the systems are stable but with an initial disturbance of 0.003m, oscillation is sustained and keeps on increasing for both

models. The reason for this behavior can be explained with the help of the values of spring force at various amplitudes of motion.

The non-linear spring force for both the models are given by

$$F = K_1X - K_3X^3 + K_5X^5 - K_7X^7;$$

A plot of F vs. X is shown in Fig. (2.6). It can be observed that as soon as amplitude of motion becomes greater than 0.0026m, the spring force becomes negative. The negative spring force is the cause for unstable response when the amplitude becomes more than 0.0026m, irrespective of elastomer models. Therefore in all further calculations, the amplitude has been restricted to less than 0.0026m.

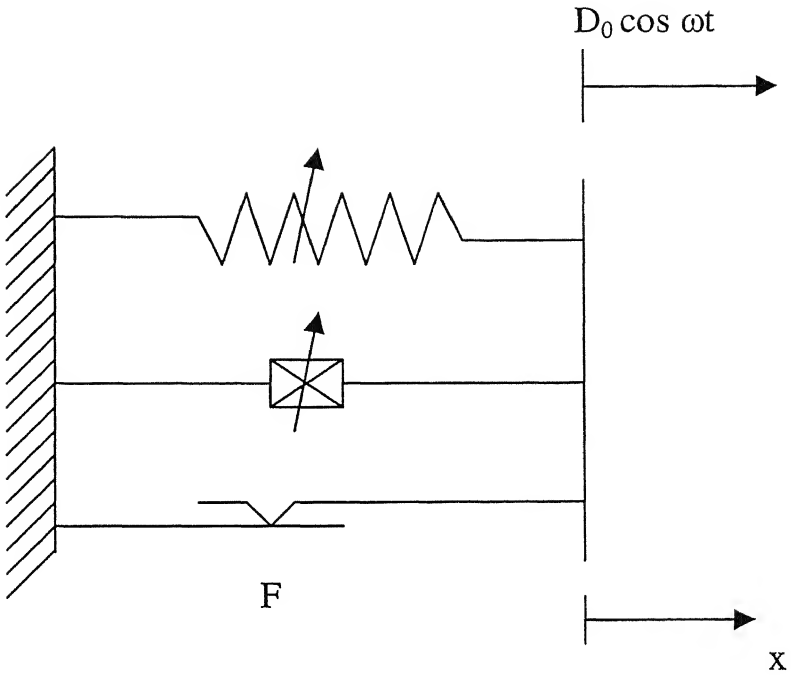

Fig 2.1. ELASTOMER MODEL

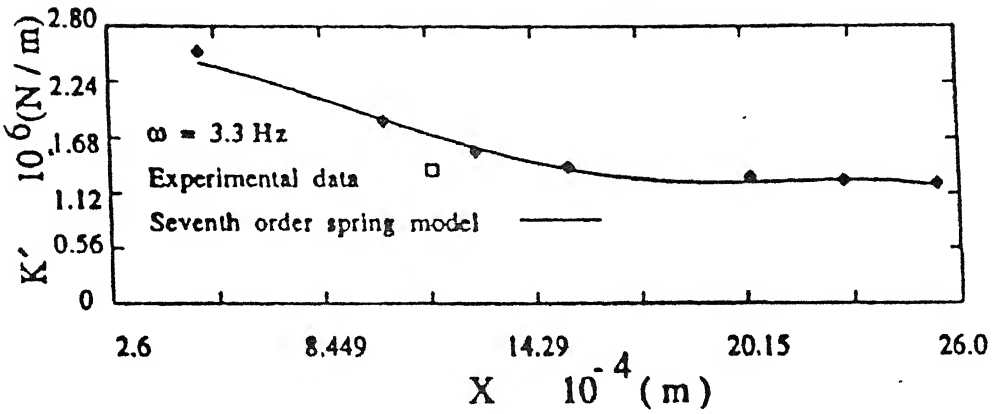

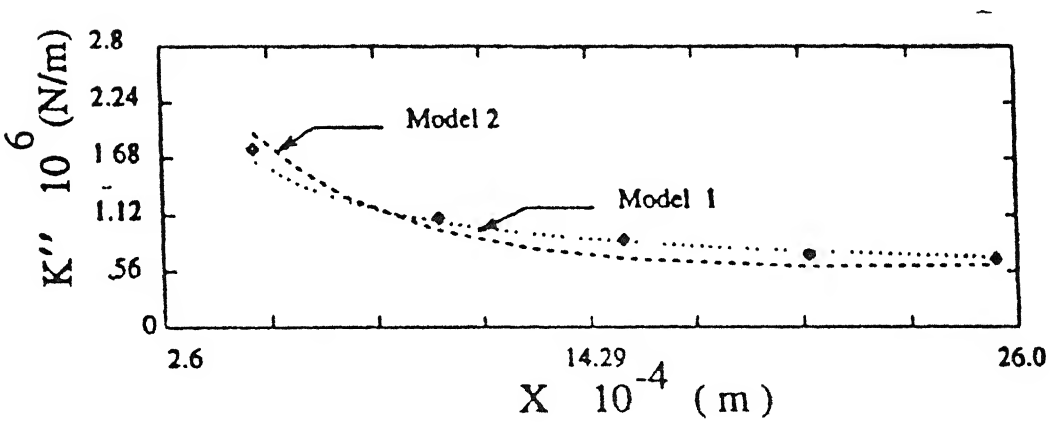

Figure 2.2 Correlation of analytical model with experimental data

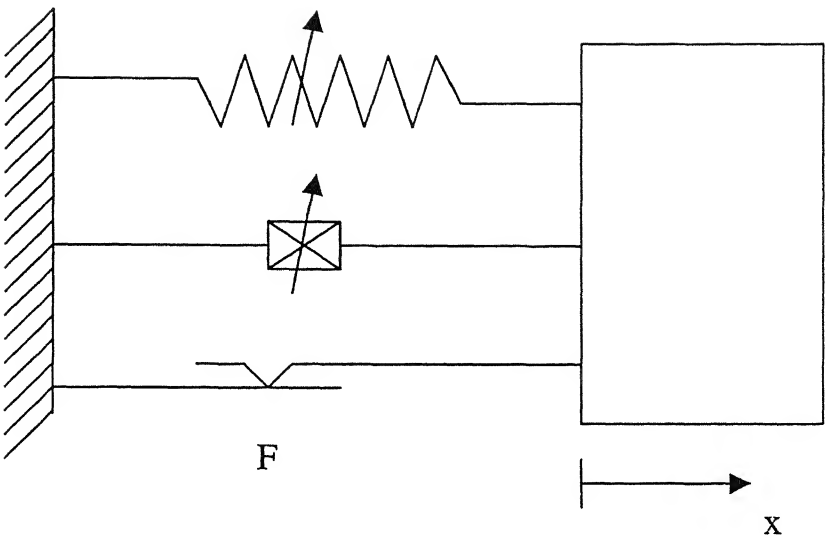

Fig 2.3. ELASTOMER MODEL WITH MASS

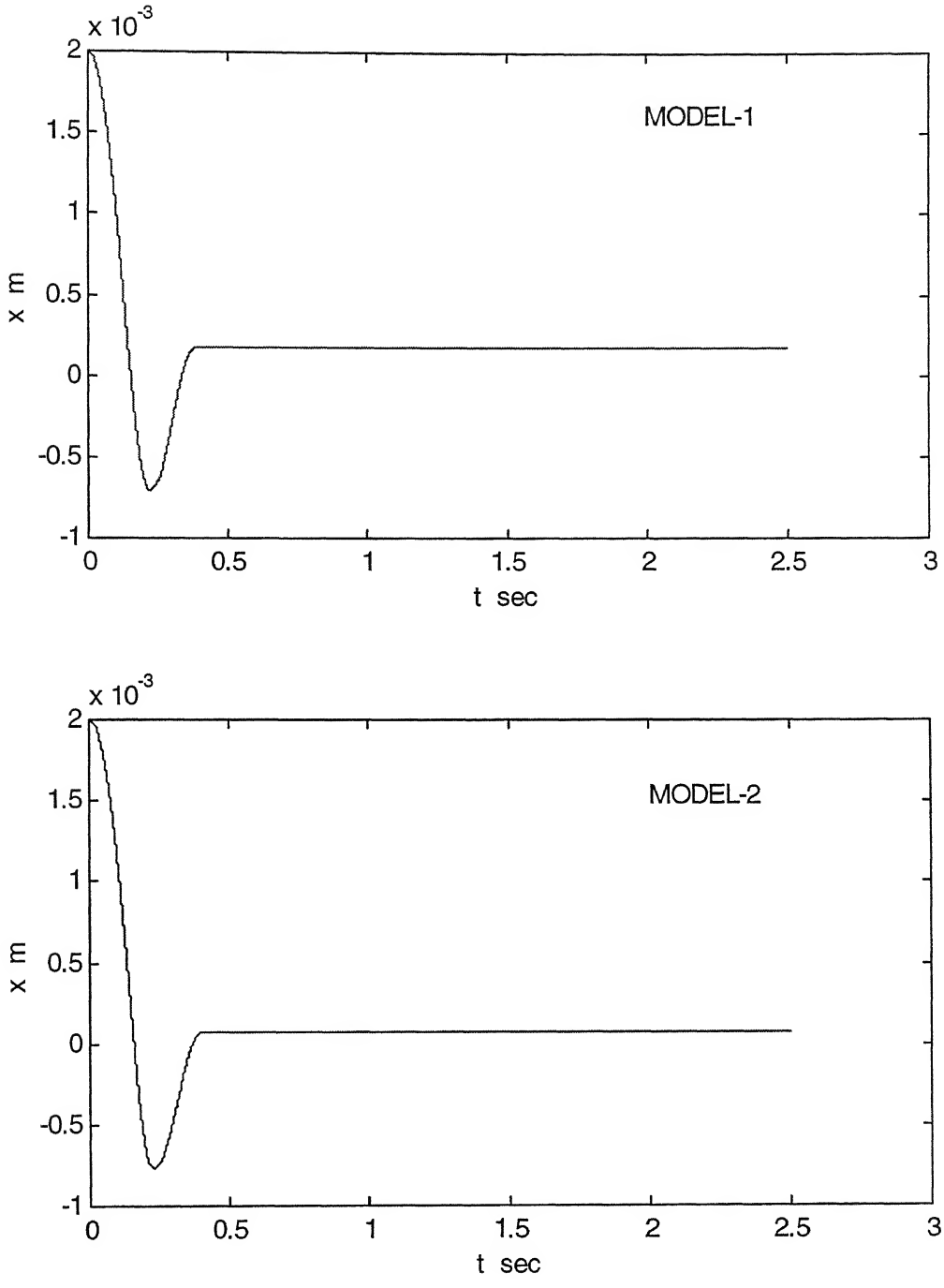

Fig. 2.4 Response of elastomer when initial disturbance is 0.002 m

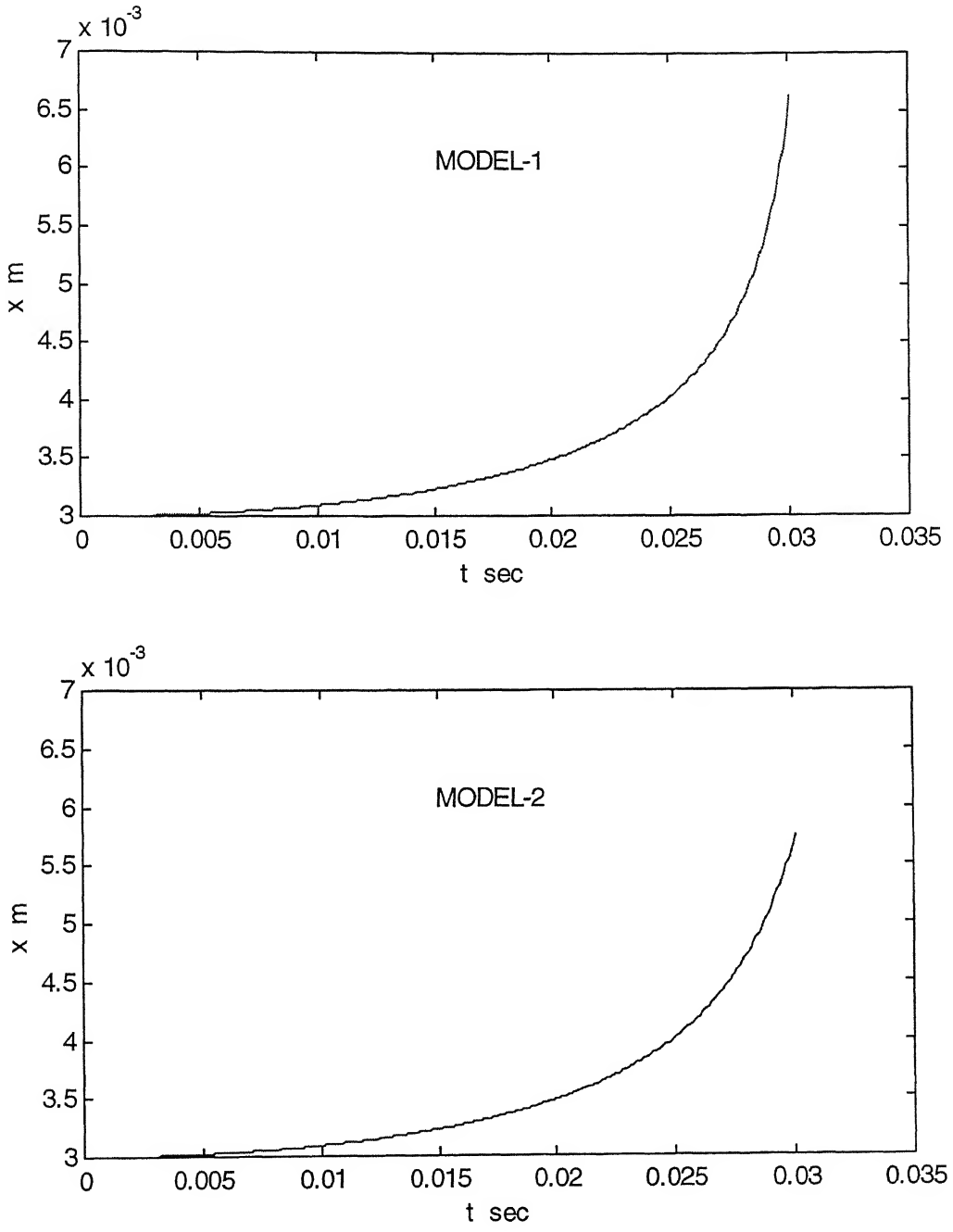

Fig. 2.5 Response for models when initial disturbance is 0.003 m

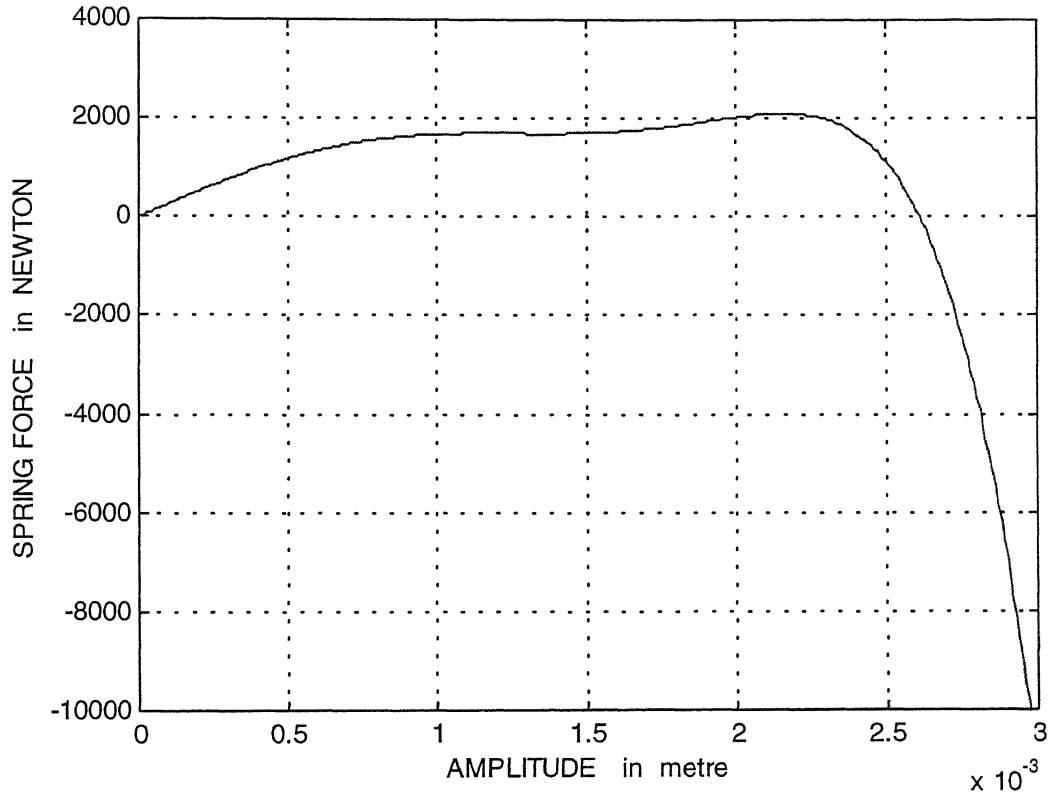

Fig 2.6 Variation of Non-linear Spring Force with Respect to Amplitude

Table 2.1. System Parameters of the Elastomer Damper

PARAMETERS	MODEL-1	MODEL -2
K_1, (N/m)	2.673989×10^6	2.673989×10^6
K_3, (N/m^3)	1.315287×10^{12}	1.315287×10^{12}
K_5; (N/m^5)	3.519586×10^{17}	3.519586×10^{17}
K_7, (N/m^7)	3.176266×10^{22}	3.176266×10^{22}
F; (N)	4.797347×10^2	8.45909×10^2
h; (N/m)	4.569120×10^5	-
h_1 ;(N/m)	-	1.44619×10^5
h_3 ;(N/m^3)	-	7.06419×10^{10}

CHAPTER-3

MOTION OF HELICOPTER BLADE IN LAG MODE

3.1. INTRODUCTION

The transient response analysis of a bearingless rotor blade requires the formulation of aeroelastic equations of motion representing coupled axial, flap-lag, and torsional motion of the blade, including the non-linear elastomer. The elastomer provides constraints in flap, lag and torsional deformation of the blade. In Chapter 2 we have seen the effect of elastomers on non-rotating systems (a very simple analysis). In this chapter we will move forward to discuss the response of the system with elastomeric lag damper in isolated lag mode, analysis of which is a little bit more complex.

3.2. THE ELASTOMERIC DAMPER MODEL IN LAG MODE

The lag mode is in-plane bending of the rotor blades. In the lag mode the elastomer is represented by both models 1 and 2. A non-linear elastomer model of section 2.2 is considered for the elastomer attached with the rotor blade. But now the non-linear spring of the section 2.2 is replaced by a non-linear torsional spring so that the restoring moment exerted by spring is

$$M_{spring} = K_1\xi - K_3\xi^3 + K_5\xi^5 - K_7\xi^7$$

Where, ξ is the angle by which the rotor blade is initially disturbed. The coulomb damping and the hysteretic damping forces of section 2.3 now become coulomb and hysteretic damping moments respectively with proper units.

3.3 EQUATION OF MOTION

A typical helicopter blade rotating about its axis is shown in Fig (3.1). The blade is idealized as a rigid rod. Cross sectional area of the blade and mass per unit length are assumed to be constant. O-O is the axis about which the blade is rotating with an angular speed of Ω. Let the mass per unit length of the blade is m. The blade is hinged at an offset of e to the axis of rotation. Let us consider a differential element of length dx at a distance of x from the hinge. The elastomer is treated as a combination of a torsional spring, which resists the motion of the blade in lag mode, together with a hysteretic and a coulomb damper. The equation of motion is derived by equating algebraic summation of all moments about the hinge to zero.

Various moments acting on the blade are:

1. Moment due to centrifugal force
2. Restoring moment exerted by the torsional spring
3. The coulomb damping moment due to elastomer opposing the motion
4. The hysteretic damping moment due to elastomer.

Moment due to centrifugal force :

The position vector of the differential element, considering point O as the origin and taking co-ordinate system as shown in Fig. (3.1), for a small initial disturbance of ξ given to the blade is given as

$$\mathbf{R} = (e + x\cos\xi)\,\mathbf{I} + x\sin\xi\,\mathbf{J}$$

And the position vector with respect to the hinge P is given as

$$\mathbf{r} = x\cos\xi\,\mathbf{I} + x\sin\xi\,\mathbf{J}$$

The centrifugal force acting on this element is

$$\mathbf{dF} = m.\,dx.\;\Omega^2\,[(e + x\cos\xi)\,\mathbf{I} + x\sin\xi\,\mathbf{J}]$$

Moment of this force about the hinge point P is given as

$$dM = \mathbf{r} \times \mathbf{dF}$$

$$= (x\cos\xi\,\mathbf{I} + x\sin\xi\,\mathbf{J}) \times$$

$$m.\,dx.\;\Omega^2.\,[(e + x\cos\xi)\,\mathbf{I} + x\sin\xi\,\mathbf{J}]$$

$$= m.\,dx.\;\Omega^2.\,[(x^2\cos\xi\sin\xi)\,\mathbf{K} - xe\sin\xi\,\mathbf{K}$$

$$- (x^2\cos\xi\sin\xi)\,\mathbf{K}]$$

$$= -m\,\Omega^2\,e\,x\sin\xi\,\mathbf{K}\,.$$

Hence, the total moment at the hinge due to the centrifugal effect is

$$M_{centri} = \int_0^l dM$$

$$= -\frac{1}{2} m\,\Omega^2\,e\,l^2\sin\xi\,\mathbf{K}\;;$$

Since, for small value of ξ

$$\sin\xi \approx \xi\;;$$

$$M_{centrifugal} = -\frac{1}{2} m\Omega^2 e l^2 \xi \qquad \text{.....(3.1)}$$

Moment due to elastomer:

Since the elastomer is assumed to be a combination of a non-linear spring, a coulomb damper and a hysteretic damper, there are three types of moments exerted by the elastomer

a) Restoring Moment due to non-linear spring

$$M_{spring} = K_1\xi - K_3\xi^3 + K_5\xi^5 - K_7\xi^7 \qquad \text{.....(3.2)}$$

b) Coulomb moment

$$M_{coloumb} = M\ \text{sgn}\ |\dot{\xi}| \qquad \text{..... ....(3.3)}$$

c) Hysteretic damping moment

$$M_{hyst} = \frac{h}{\omega}\dot{\xi} \quad \text{.....(3.4}a\text{)} \qquad \text{For model 1}$$

$$= \frac{h_3}{\omega^3}\dot{\xi}^3 - \frac{h_1}{\omega}\dot{\xi} \quad \text{.....(3.4}b\text{)} \qquad \text{For model 2}$$

Total moment about the hinge

The moment of inertia of the beam about the hinge is given as

$$I = \frac{1}{3}ml^3 \quad \text{.....(3.5)}$$

For Model 1 of the elastomer, taking moments about hinge

$$I\ddot{\xi} + K_1\xi - K_3\xi^3 + K_5\xi^5 - K_7\xi^7 + M\,\text{sgn}\,|\dot{\xi}| + \frac{h}{\omega}\dot{\xi} + \frac{1}{2}m\Omega^2 el^2\xi = 0$$

Taking linear terms in ξ together

$$\ddot{\xi} + \frac{1}{I}\left(K_1 + \frac{3}{2}\frac{Ie\Omega^2}{l}\right)\xi + \frac{1}{I}\left(-K_3\xi^3 + K_5\xi^5 - K_7\xi^7 + M\,\text{sgn}\,|\dot{\xi}| + \frac{h}{\omega}\dot{\xi}\right) = 0$$

.....(3.6)

Similarly, for Model 2, equation of motion can be written as

$$\ddot{\xi} + \frac{1}{I}\left(K_1 + \frac{3}{2}\frac{Ie\Omega^2}{l}\right)\xi + \frac{1}{I}\left(-K_3\xi^3 + K_5\xi^5 - K_7\xi^7 + M\,\text{sgn}\,|\dot{\xi}| - \frac{h_1}{\omega}\dot{\xi} + \frac{h_3}{\omega^3}\dot{\xi}^3\right)$$

$$= 0 \quad \text{.....(3.7)}$$

Equation in non-dimensional form can be obtained by putting

$$\ddot{\xi} = \Omega^2\frac{d^2\xi}{d(\Omega t)^2} = \Omega^2\xi'' \quad \text{.....(3.8)}$$

3.4. RESULTS AND DISCUSSION

The value of hinge offset and blade length are taken from practical data, which is 0.8 m and 5.2 m respectively. The speed of rotor Ω is taken as 32 rad/sec. The moment of inertia of the blade about hinge (I) is taken by assuming the first natural frequency of the blade as 3.3 Hz and taking stiffness of the blade as that of linear term only which is calculated from equation (3.7) as:

$$\frac{1}{I}\left(K_1 + \frac{3}{2}\frac{Ie\Omega^2}{l}\right) = \omega_n{}^2$$

Or,

$$\frac{K_1}{I\Omega^2} + \frac{3}{2}\frac{e}{l} = \left(\frac{\omega_n}{\Omega}\right)^2$$

Which gives the value of I as 13811 Kg-m^2 Equation (3.7) is a non-linear differential equation, which can be solved by numerical integration techniques. In the present work, *fourth order Runge-Kutta* method is adopted to solve the non-linear equations. Solving equation of motion numerically using a time step of 0.001, we get the responses of the system as shown in Fig. (3.2) and Fig. (3.3) for two different input conditions. Figure (3.2) shows the responses of the system for both the models when initial disturbance given as input is taken as 0.0015 and Fig. (3.3) shows the responses of the system for both the models when initial disturbance given as input is taken as 0.0025. In both cases, the initial velocity is taken as zero. It is observed from Fig. (3.2) and Fig. (3.3) that the system is stable and oscillations continuously decay for both the models for both input conditions. Also, both models predict identical behavior and there is no any evidence of the occurrence of limit cycle oscillations.

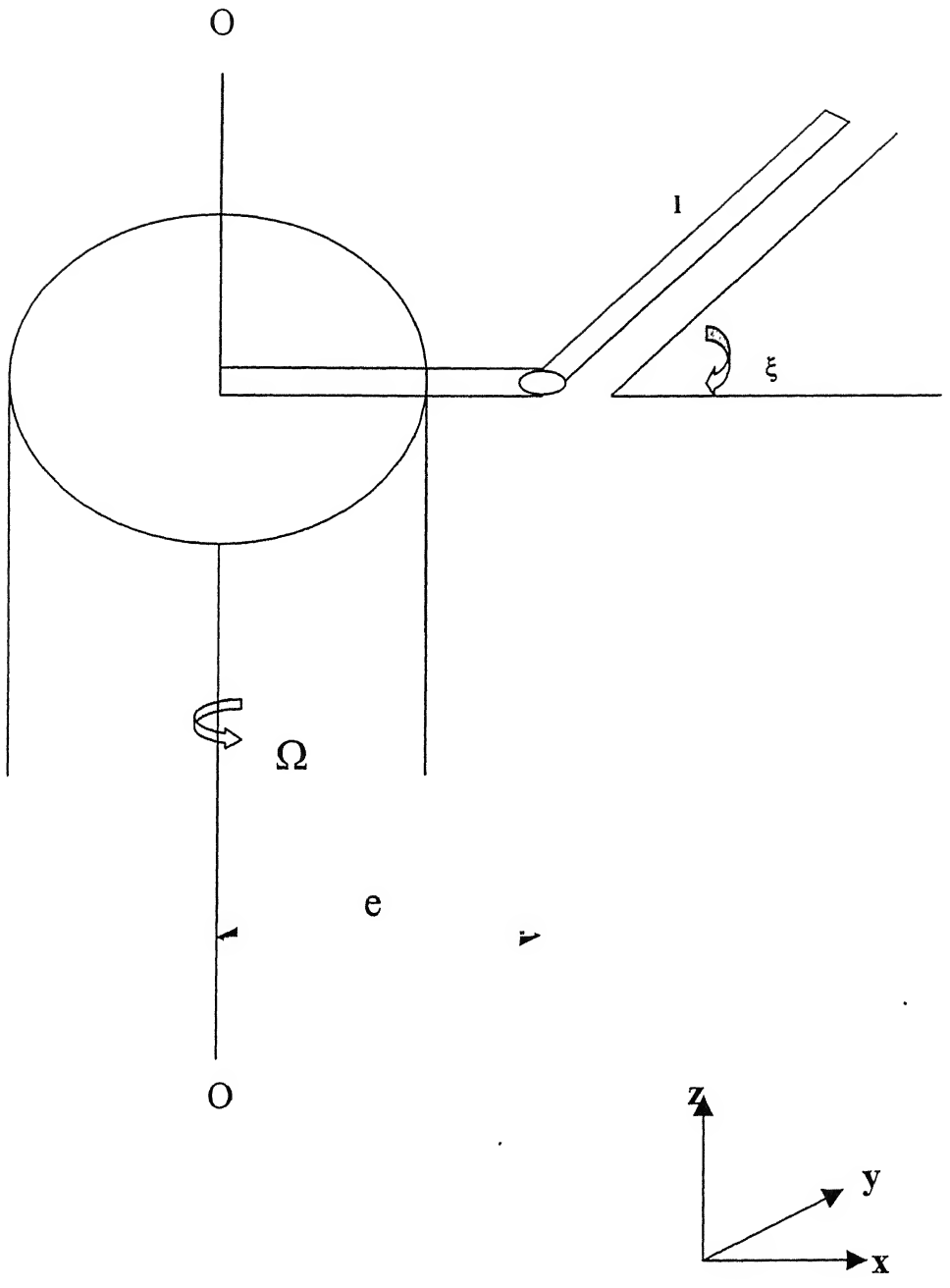

Figure 3.1 A Rotating Helicopter Blade

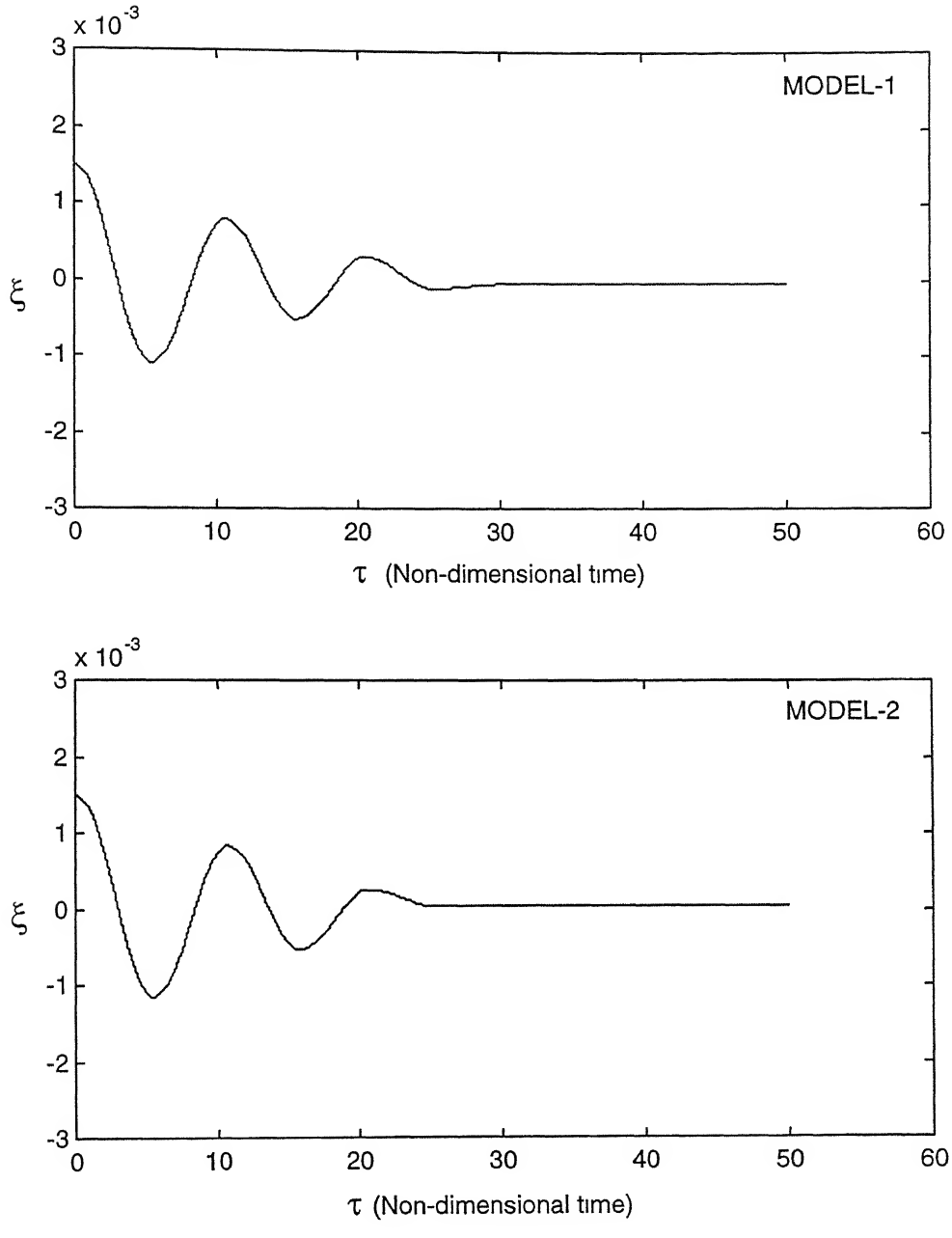

Figure 3.2. Response of the Systems in Uncoupled Lag mode with for initial disturbance, ξ_0=0.0015.

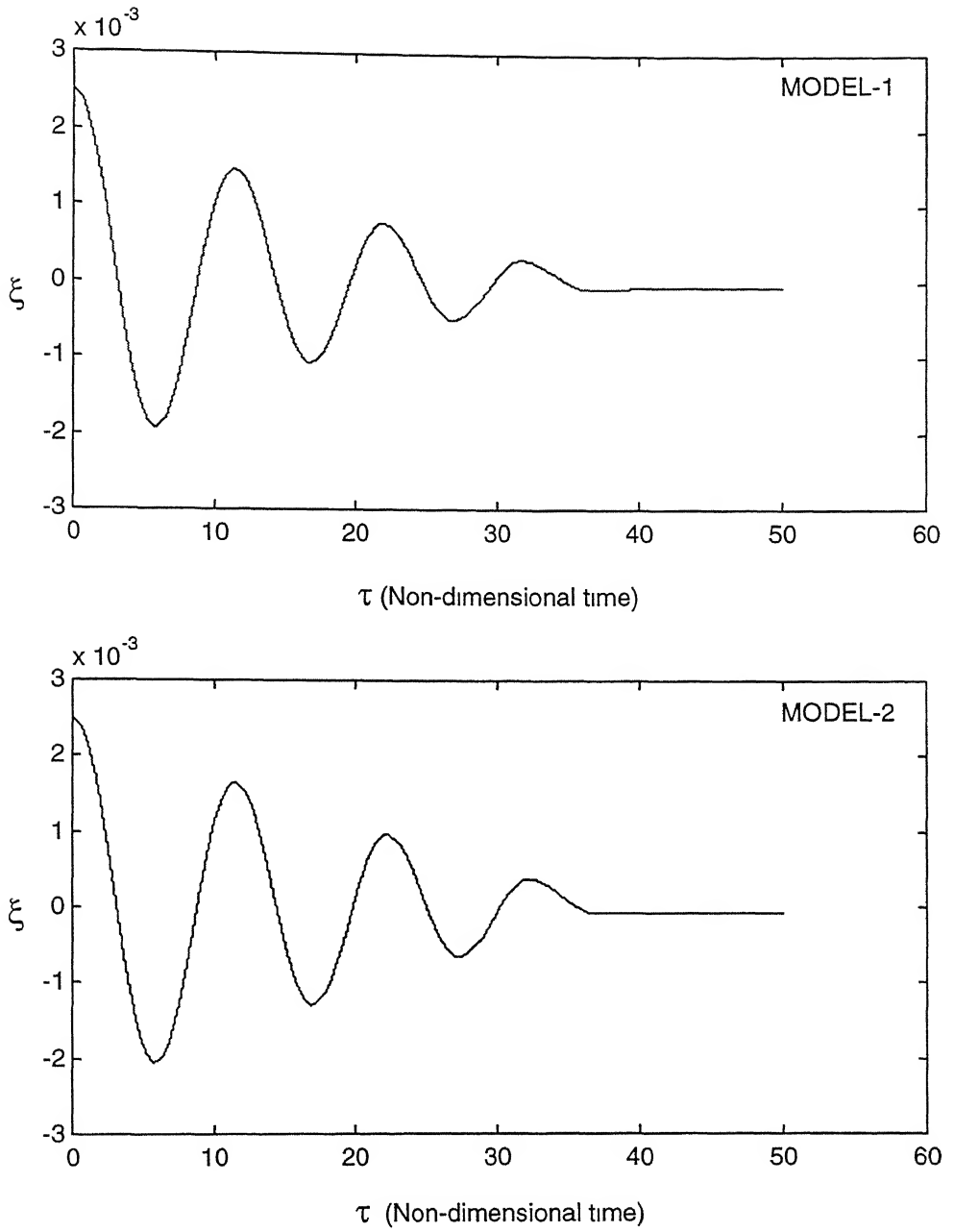

Figure 3.3. Response of the Systems in Uncoupled Lag mode for initial disturbance, $\xi_0 = 0.0025$.

CHAPTER - 4

MOTION OF HELICOPTER BLADE IN FLAP-LAG COUPLED MODE

4.1. INTRODUCTION

Many researchers have worked on the phenomena of limit cycle oscillation behavior of the rotor blades due to elastomer non-linearity. Ormiston et al. [10] considered an elastomer model in which the damping force was assumed to be proportional to a linear combination of different powers of velocity (powers of ½, 1, 2 and 3). Using this non-linear elastomer model, they showed the presence of limit cycle oscillation for both hingeless and bearingless rotor blade configurations. It was also pointed out that there was no limit cycle when the elastomer damping is taken as linear. In this chapter the presence of limit cycle behavior in rotor blades with both elastomer damper models will be discussed.

In helicopter rotors, blades are attached to the rotor with some precone. The precone angle is practically so chosen that during the flight while rotating, the blades come at horizontal position. So it is essential to analyze the behavior of limit cycle in coupled flap-lag mode including the effect of precone.

4.2 EQUATION OF MOTION IN COUPLED FLAP-LAG MODE

Since the elastomer data are available only for lag mode, the elastomer is represented by a very stiff linear spring in the flap mode. In the lag mode the elastomer is represented by both models 1 and 2. A schematic diagram of the rotor blade rotating in coupled flap-lag mode is shown in Fig. 4.1. Let us consider

an element of length dr at a distance of r from the hinge. The blade is assumed to be a rigid rod. The mass per unit length of the blade is m and the blade is assumed to be of uniform cross-section. Treating O as the origin and considering model 1 first, the position vector of an element is given as

$$\vec{R} = (e + r\cos\beta\cos\xi)\vec{I} + r\cos\beta\sin\xi\,\vec{J} + r\sin\beta\,\vec{K} \quad \ldots\ldots\ldots (4.1)$$

Absolute velocity of the element is given as

$$\vec{V} = \Omega\,\vec{K} \times \vec{R} + \dot{\vec{R}} \ .$$

Or,

$$\vec{V} = -\left(\Omega r\cos\beta\sin\xi + r\dot{\beta}\sin\beta\cos\xi + r\dot{\xi}\cos\beta\sin\xi\right)\vec{I} + \left(\Omega e + \Omega r\cos\beta\cos\xi + r\dot{\xi}\cos\beta\cos\xi - r\dot{\beta}\sin\beta\sin\xi\right)\vec{J} + r\dot{\beta}\cos\beta\,\vec{K} \quad \ldots\ldots\ldots (4.2)$$

$$V^2 = \vec{V}\cdot\vec{V} = (-r\dot{\beta}\sin\beta\cos\xi - r\dot{\xi}\cos\beta\sin\xi - \Omega r\cos\beta\sin\xi)^2 + (\Omega e + \Omega r\cos\beta\cos\xi + r\dot{\xi}\cos\beta\cos\xi - r\dot{\beta}\sin\beta\sin\xi)^2 + (r\dot{\beta}\cos\beta)^2$$

$$= r^2\dot{\beta}^2[\sin^2\beta(\cos^2\xi + \sin^2\xi) + \cos^2\beta] + \Omega^2e^2 + r^2\dot{\xi}^2\cos^2\beta(\sin^2\xi + \cos^2\xi) + \Omega^2r^2\cos^2\beta(\sin^2\xi + \cos^2\xi) + 2\Omega r^2\dot{\xi}\cos^2\beta(\sin^2\xi + \cos^2\xi) + 2\Omega^2er\cos\beta\cos\xi + 2\Omega er\dot{\xi}\cos\beta\cos\xi - 2\Omega er\dot{\beta}\sin\beta\sin\xi$$

Or,

$$V^2 = r^2\dot{\beta}^2 + \Omega^2 e^2 + r^2\dot{\xi}^2\cos^2\beta + \Omega^2 r^2\cos^2\beta$$
$$+ 2\Omega r^2\dot{\xi}\cos^2\beta + 2\Omega^2 er\cos\beta\cos\xi$$
$$+ 2\Omega er\dot{\xi}\cos\beta\cos\xi - 2\Omega er\dot{\beta}\sin\beta\sin\xi \quad \text{.....(4.3)}$$

Total kinetic energy,

$$T = \frac{1}{2}\int_0^l mdr.V^2 \quad \text{.....(4.4)}$$

Or,

$$T = \frac{1}{2}m\int_0^l (r^2\dot{\beta}^2 + \Omega^2 e^2 + r^2\dot{\xi}^2\cos^2\beta + \Omega^2 r^2\cos^2\beta$$
$$+ 2\Omega r^2\dot{\xi}\cos^2\beta + 2\Omega^2 er\cos\beta\cos\xi$$
$$+ 2\Omega er\dot{\xi}\cos\beta\cos\xi - 2\Omega er\dot{\beta}\,\text{sin}\,\beta\sin\xi)dr$$

Or,

$$T = \frac{1}{6}ml^3\dot{\beta}^2 + \frac{1}{2}m\Omega^2 e^2 l + \frac{1}{6}ml^3\dot{\xi}^2\cos^2\beta$$
$$+ \frac{1}{6}m\Omega^2 l^3\cos^2\beta + \frac{1}{3}m\Omega l^3\dot{\xi}\cos^2\beta + \frac{1}{2}ml\Omega^2 e\cos\beta\cos\xi$$
$$+ \frac{1}{2}m\Omega el^2\dot{\xi}\cos\beta\cos\xi - \frac{1}{2}m\Omega\ el^2\dot{\beta}\sin\beta\sin\xi \quad \text{.....(4.5)}$$

Potential energy of the spring is given as

$$U = \int_0^\xi \left(K_1\xi - K_3\xi^3 + K_5\xi^5 - K_7\xi^7\right)d\xi$$

Or,

$$U = \frac{1}{2}K_1\xi^2 - K_3\frac{1}{3}\xi^4 + K_5\frac{1}{5}\xi^6 - K_7\frac{1}{7}\xi^8 \quad \text{.....(4.6)}$$

Now applying Lagrange's equation in lag mode degree of freedom

$$\frac{d}{dt}\left(\frac{\partial T}{\partial \dot{\xi}}\right)-\frac{\partial T}{\partial \xi}+\frac{\partial U}{\partial \xi}=Q_{NC} \text{ ....(4.7)}$$

Where Q_{NC} is the non-conservative force associated with the lag mode. From equations (4.7) to (4.9) we get the equation of motion in lag mode as

$$\frac{1}{3}\mathrm{ml}^3\ddot{\xi}-\frac{2}{3}ml^3\dot{\beta}\dot{\xi}\beta-\frac{2}{3}m\Omega l^3\beta\dot{\beta}+\frac{1}{2}m\Omega^2 el^2\xi$$
$$+K_1\xi-K_3\xi^3+K_5\xi^5-K_7\xi^7+F\,\mathrm{sgn}\,|\dot{\xi}|+\frac{h}{\omega}\dot{\xi}=0$$

Neglecting the third order terms we get the equation of motion in the lag mode motion as

$$\frac{1}{3}\mathrm{ml}^3\ddot{\xi}-\frac{2}{3}m\Omega l^3\beta\dot{\beta}+\frac{1}{2}m\Omega^2 el^2\xi$$
$$+K_1\xi-K_3\xi^3+K_5\xi^5-K_7\xi^7+F\,\mathrm{sgn}\,|\dot{\xi}|+\frac{h}{\omega}\dot{\xi}=0 \text{.....(4.8)}$$

or,

$$I\ddot{\xi}-2I\Omega\dot{\beta}\beta+\left(\frac{3}{2}\frac{e}{l}I\Omega^2+K_1\right)\xi-K_3\xi^3+K_5\xi^5-K_7\xi^7$$
$$+F\,\mathrm{sgn}\,|\dot{\xi}|+\frac{h}{\omega}\dot{\xi}=0 \text{.....(4.9)}$$

Where, I is the moment of inertia of the blade about hinge

$$I=\frac{1}{3}ml^3$$

Equation in non-dimensional form can be obtained by putting

$$\ddot{\xi}=\Omega^2\frac{d^2\xi}{d(\Omega t)^2}=\Omega^2\xi'' \text{..... ....(4.10)}$$

and

$$\ddot{\beta}=\Omega^2\frac{d^2\beta}{d(\Omega t)^2}=\Omega^2\beta'' \text{..... ....(4.11)}$$

From equations (4.9), (4.10) and (4.11), equation of motion becomes

$$\xi'' - 2\beta\beta' + \left(\frac{3}{2}\frac{e}{l} + \frac{K_1}{I\Omega^2}\right)\xi + \frac{1}{I\Omega^2}\left(-K_3\xi^3 + K_5\xi^5 - K_7\xi^7 + F\,\mathrm{sgn}\,|\dot{\xi}| + \frac{h}{\omega}\Omega\xi'\right) = 0 \quad \text{.....(4.12)}$$

Now applying Lagrange's equation in flap mode of vibration we get the equation of motion in flap direction as

$$\frac{d}{dt}\left(\frac{\partial T}{\partial \dot{\beta}}\right) - \frac{\partial T}{\partial \beta} + \frac{\partial U}{\partial \beta} = Q_{NC\beta} \quad \text{.....(4.13)}$$

Where $Q_{NC\beta}$ is the non-conservative force associated with the flap mode of vibration.

From equations (4.5), (4.6) and (4.13), the equation of motion in flap direction is obtained as

$$\frac{1}{3}\mathrm{m}l^3\ddot{\beta} + \frac{1}{3}ml^3\dot{\xi}^2\beta + \frac{1}{3}m\Omega l^3\dot{\xi}\beta + \frac{1}{3}m\Omega^2 l^3\beta + \frac{1}{2}m\Omega^2 el^2\beta = 0$$

Neglecting the third order term, equation of motion reduces to

$$\frac{1}{3}\mathrm{m}l^3\ddot{\beta} + \frac{1}{3}m\Omega l^3\dot{\xi}\beta + \frac{1}{3}m\Omega^2 l^3\beta + \frac{1}{2}m\Omega^2 el^2\beta = 0 \quad \text{.....(4.14)}$$

From equations (4.10), (4.11) and (4.14), equation in non-dimensional form for flap motion becomes

$$\beta'' + \beta\xi' + \left(1 + \frac{3}{2}\frac{e}{l}\right)\beta = 0 \quad \text{.....(4.15)}$$

Similarly, for model 2 the equation of motion in lag is given as

$$\xi'' - 2\beta\beta' + \left(\frac{3}{2}\frac{e}{l} + \frac{K_1}{I\Omega^2}\right)\xi + \frac{1}{I\Omega^2}\left(-K_3\xi^3 + K_5\xi^5 - K_7\xi^7 + F\,\mathrm{sgn}\,|\dot{\xi}| - \frac{h_1}{\omega}\Omega\xi' + \frac{h_3}{\omega^3}\Omega^3\xi'^3\right) = 0. \quad \text{(4.16)}$$

And the equation of motion in flap will be same as that of model 1 i.e.

$$\beta'' + \beta\xi' + \left(1 + \frac{3}{2}\frac{e}{l}\right)\beta = 0 \quad \text{.....(4.17)}$$

If flap mode is provided with a damping factor ζ then the equation of motion in flap will be

$$\beta'' + \beta\xi' + \left(1 + \frac{3}{2}\frac{e}{l}\right)\beta + 2\zeta\frac{\omega_n}{\Omega}\beta' = 0 \quad \text{.....(4.18)}$$

4.3 RESULTS AND DISCUSSION.

The values of e, l, Ω and I are taken same as that of chapter 3, which are 0.8 m, 5.2 m, 32 rad/sec and 13811 Kg-m^2, respectively. Using equations (4.12) and (4.15) the transient response characteristics of the rotor blade in coupled flap-lag mode are obtained for elastomer Model 1 and using equations (4.16) and (4.17) the transient response characteristics of the rotor blade in coupled flap-lag mode are obtained for elastomer Model 2. These equations are non-linear differential equations, which can be solved by numerical integration technique. As in chapter 3, in this chapter also equations are solved using *fourth order Runge-Kutta method.* A time step of 0.001 is used in solving the equations.

Figure (4.2) shows the response of the system when an initial disturbance of 0.002 is given in lag direction for Model 1, i.e., no initial disturbance is given in flap direction. Figure (4.3) shows the response of the system under the same initial condition for Model 2. It is observed from Fig. (4.2) that the oscillation in lag mode is damping out but the flap mode remains undisturbed. Exactly same result can be observed from Fig. (4.3) for Model 2. Hence, it can be inferred that there is no effect of coupling from lag mode to flap mode i.e., there is no transfer of energy from lag mode to flap mode for both the models.

Now, the response characteristics of elastomer models are obtained for disturbing flap initially. Figure 4.4 shows the response of Model 1 when an initial input of 0.04 is given to flap direction. Figure 4.5 shows the response of the system for Model 2 when an initial disturbance of 0.04 is given to flap direction. It is observed from Fig. (4.4) that disturbing flap initially, due to the coupling

effect lag mode also gets excited. The lag mode oscillation soon settles down to a limit cycle oscillation. But the flap mode remains oscillating with the same amplitude (although the amplitude of flap is decreasing, but the damping in the flap mode is so less that we can assume it as oscillating with almost the same amplitude). Same result is observed from Fig. (4.5) for Model 2. Also it is observed from Fig. (4.4) and Fig. (4.5) that within a short time, the lag response settles down to a stable limit cycle for both models. Although, model 1 has no nonlinear damping terms it still exhibits limit cycle oscillation. It is due to the flap-lag coupling. Due to coupling, a Coriollis term containing the product of β and $\dot{\beta}$ appears in the equation of motion which may be positive or negative depending upon β and $\dot{\beta}$ and thus causing the limit cycle oscillation.

To control the limit cycle oscillations, a small amount of damping is inserted in the flap mode. Equation (4.17) is the equation of motion in flap direction with a damping of ζ. Solving equations (4.12) and (4.18) numerically, the response of the elastomer Model 1 after incorporating the flap damping is obtained. Figure (4.6) shows the response of the elastomer model 1 with 10% flap damping, which is disturbed initially by 0.04 in flap direction. From Fig. (4.6) one can observe that inclusion of a little damping in the flap direction eliminates the limit cycle oscillation in the lag mode. The lag mode stabilizes and the flap mode also damps out. Solving equations (4.15) and (4.18) numerically we get the response of elastomer Model 2 after incorporating a damping in the flap direction. Figure (4.7) shows the response of Model 2, having initial disturbance of 0.04 in flap direction and including 10% damping in the flap mode. In this case also, oscillations in both flap and lag modes damp out very rapidly. Hence, it can be inferred that inserting a very small amount of damping in the flap direction (even 1%) the oscillations in both flap and lag both modes decay very rapidly for both the models.

The blades are always attached with the rotor hub at some pre-cone. The pre-cone angle is chosen by the manufacturer from certain practical considerations.. To get the equations of motion with precone, we simply substitute β by $(\beta_p+\beta_1)$ and $\ddot{\beta}$

by $\ddot{\beta}_1$, where β_p is the angle of precone provided initially and β_1 is the disturbance from the precone state. Figure (4.8) and Fig. (4.9) show the responses of the elastomer models having precone of 0.03. An initial disturbance of 0.01 is given in flap direction. It can be observed that in the lag mode, the system exhibits limit cycle oscillation and in the flap mode it is oscillating with a constant amplitude of 0.08 about the mean position of –0.03. Figure (4.10) and Fig. (4.11) show the responses of the elastomer models having precone and flap damping. One can observe that the flap and the lag oscillations are damping out very rapidly for both models. But the flap mode settles down to –0.03 (i.e. neagative of the precone angle). Therefore, it can be inferred that, flap and lag both modes exhibit rapid decay with the flap mode settling at negative of the precone angle position (i.e., the position when blade becomes horizontal).

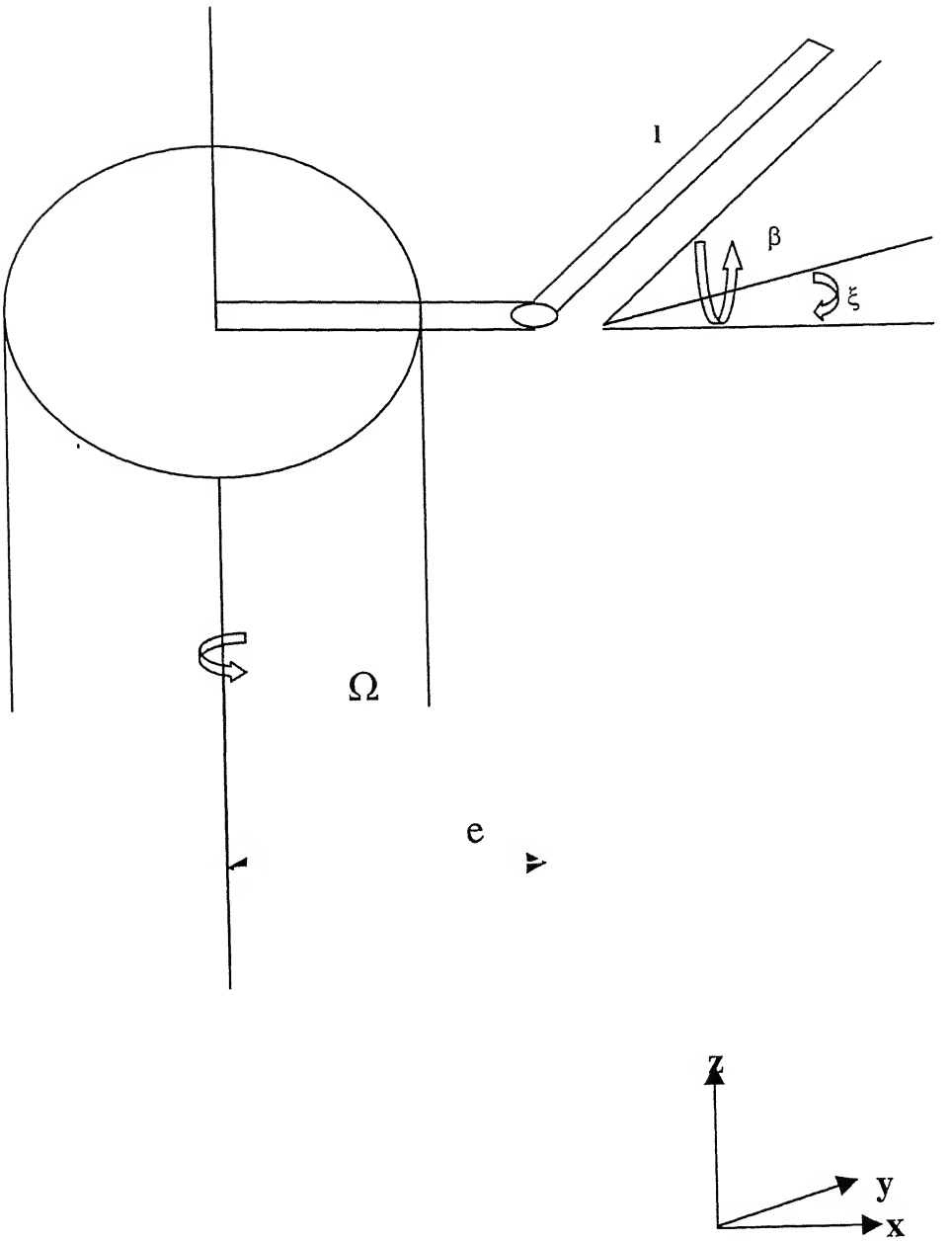

Figure 4.1. A Rotating Helicopter Rotor Blade

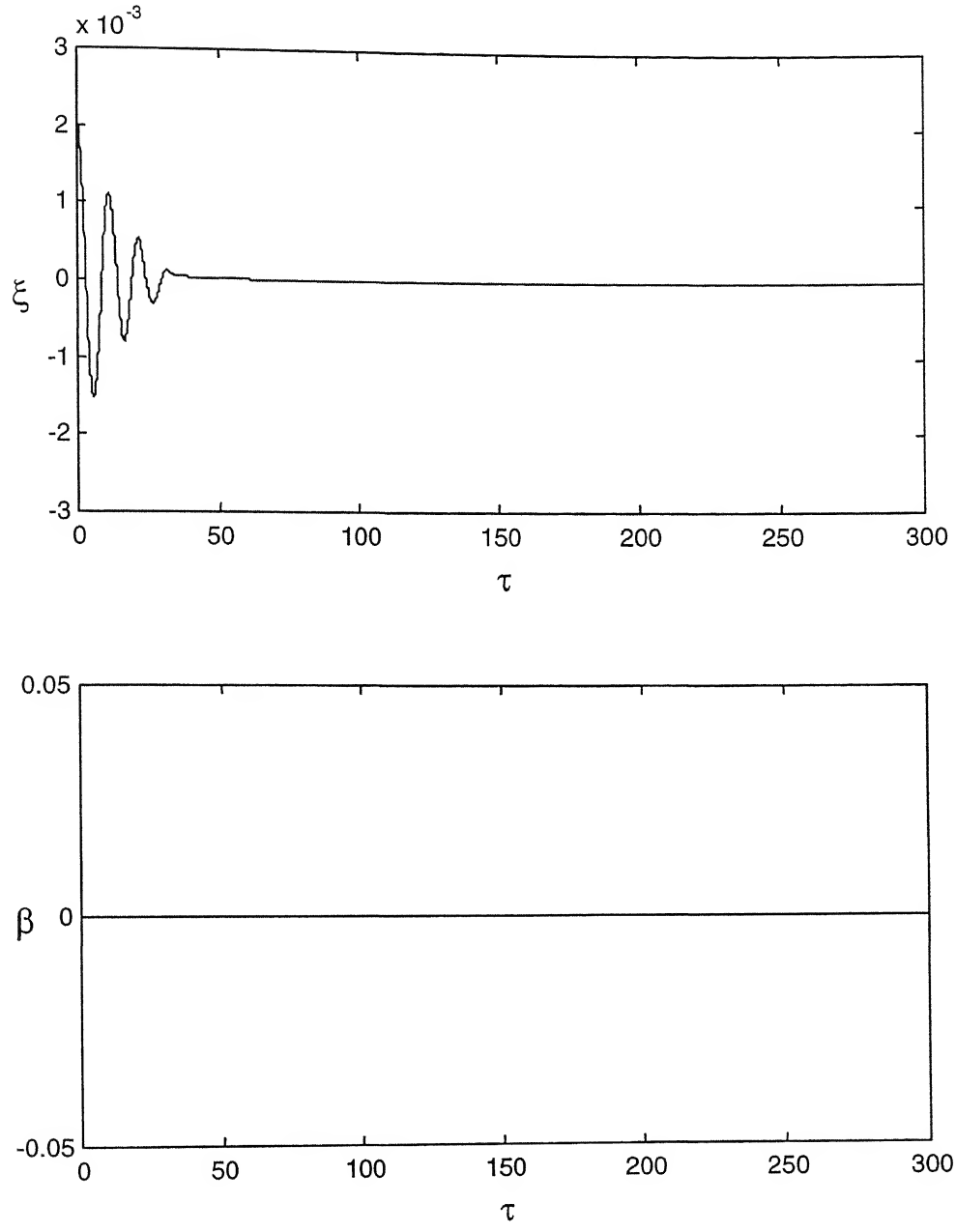

Fig 4.2. Response of Elastomer Model 1 With Initial Disturbance in Lag Direction

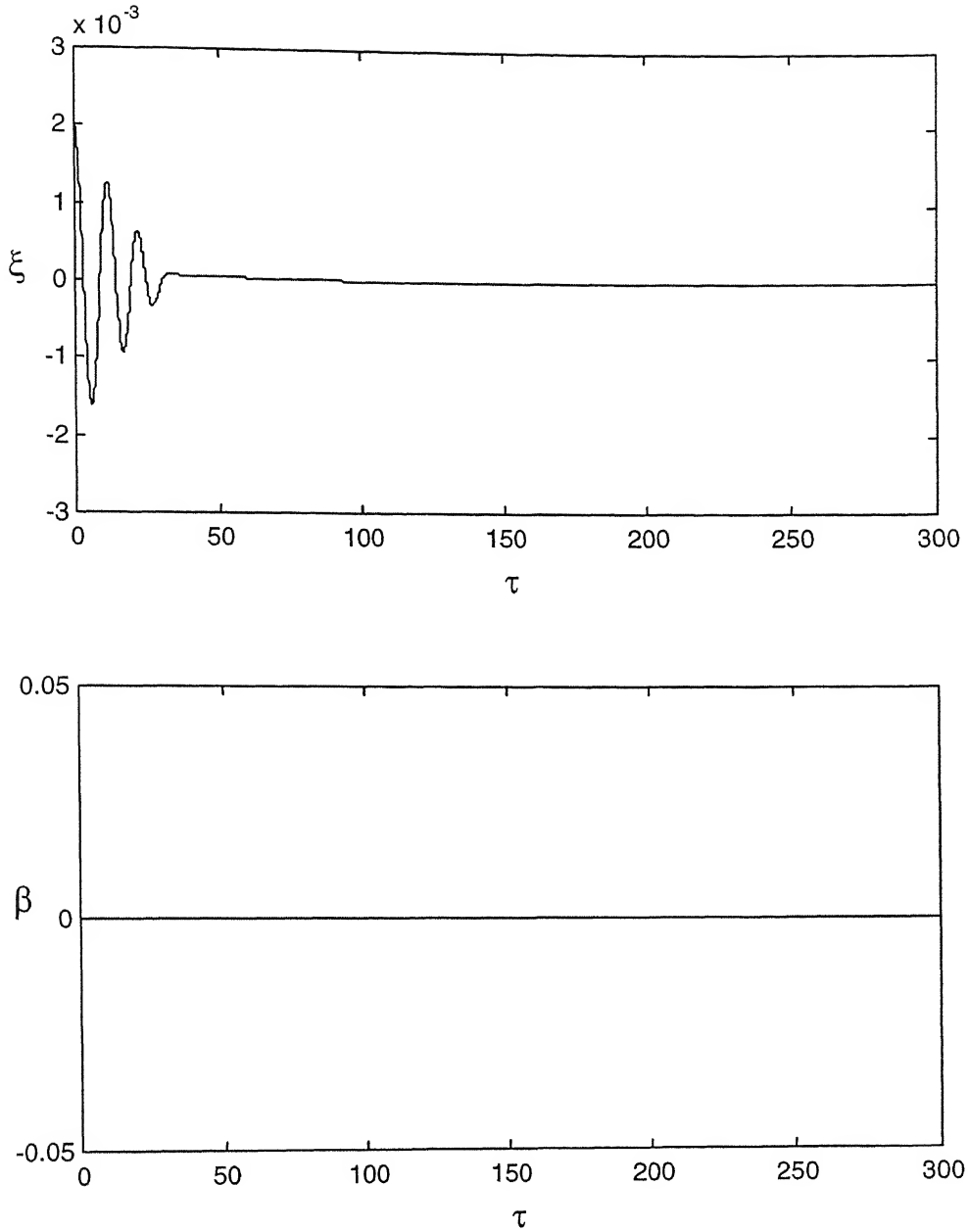

Fig 4.3. Response of Elastomer Model 2 With Initial Disturbance in Lag Direction

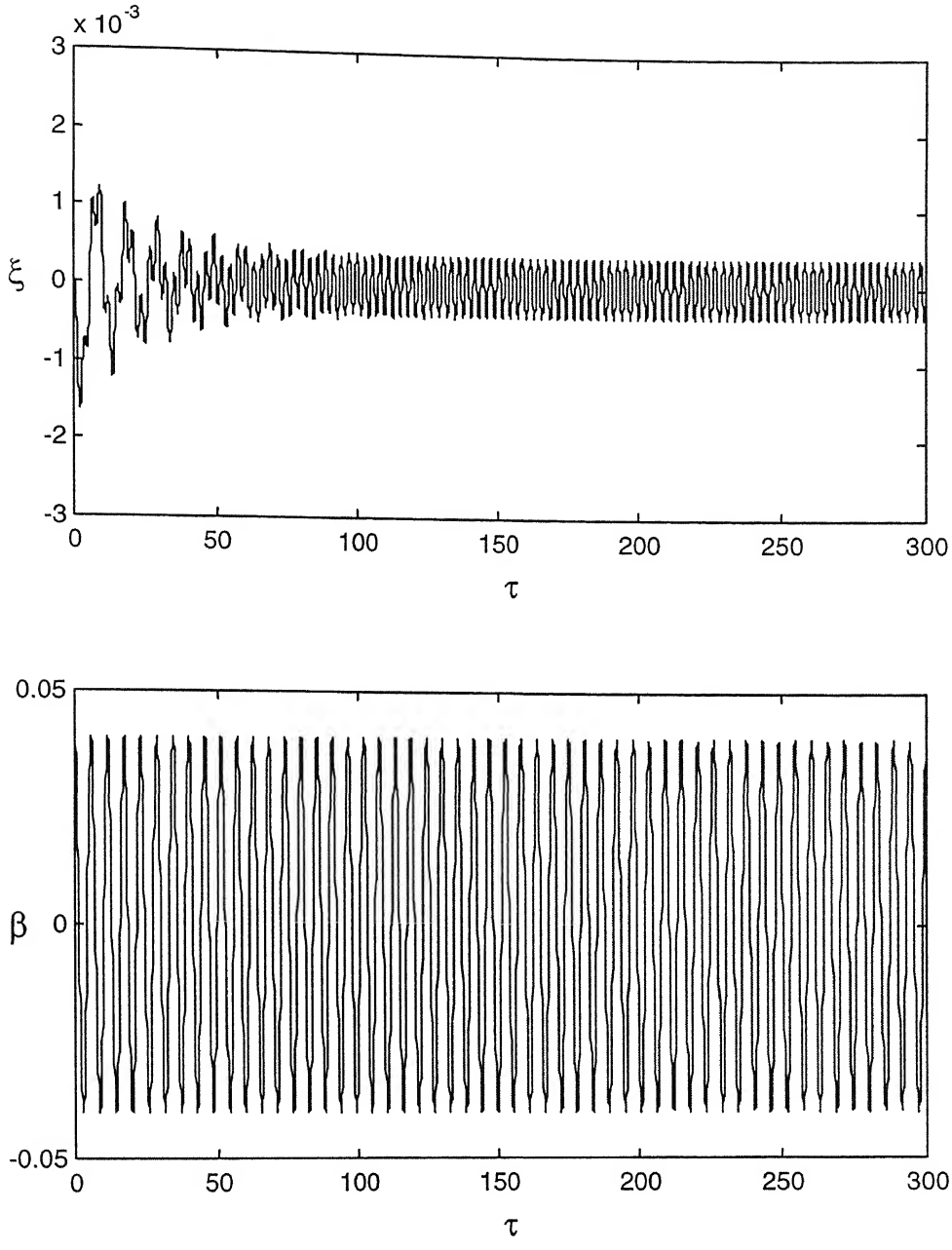

Fig 4.4. Response of Elastomer Model 1 With Initial Disturbance in Flap Direction

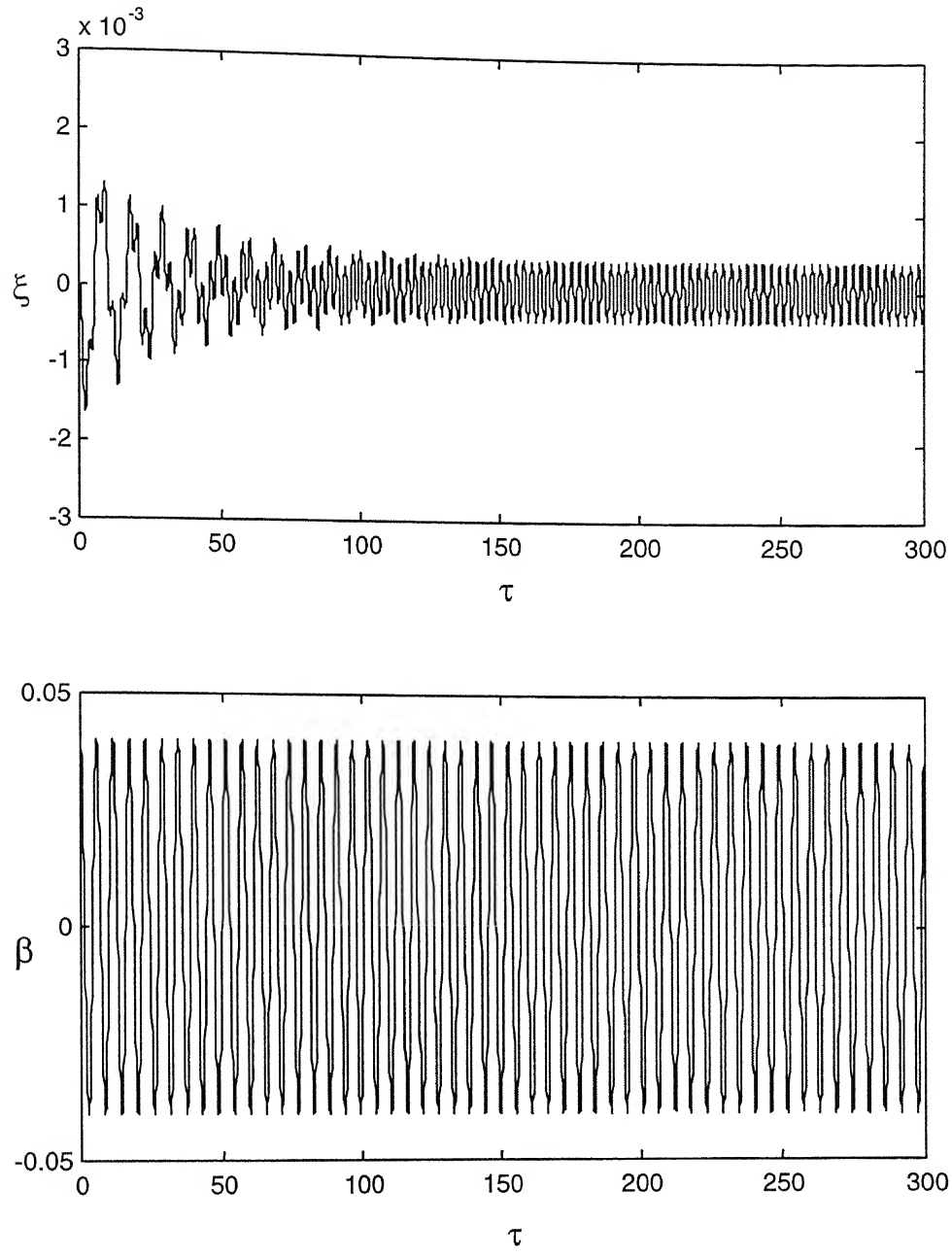

Fig 4.5. Response of Elastomer Model 2 With Initial Disturbance in Flap Direction

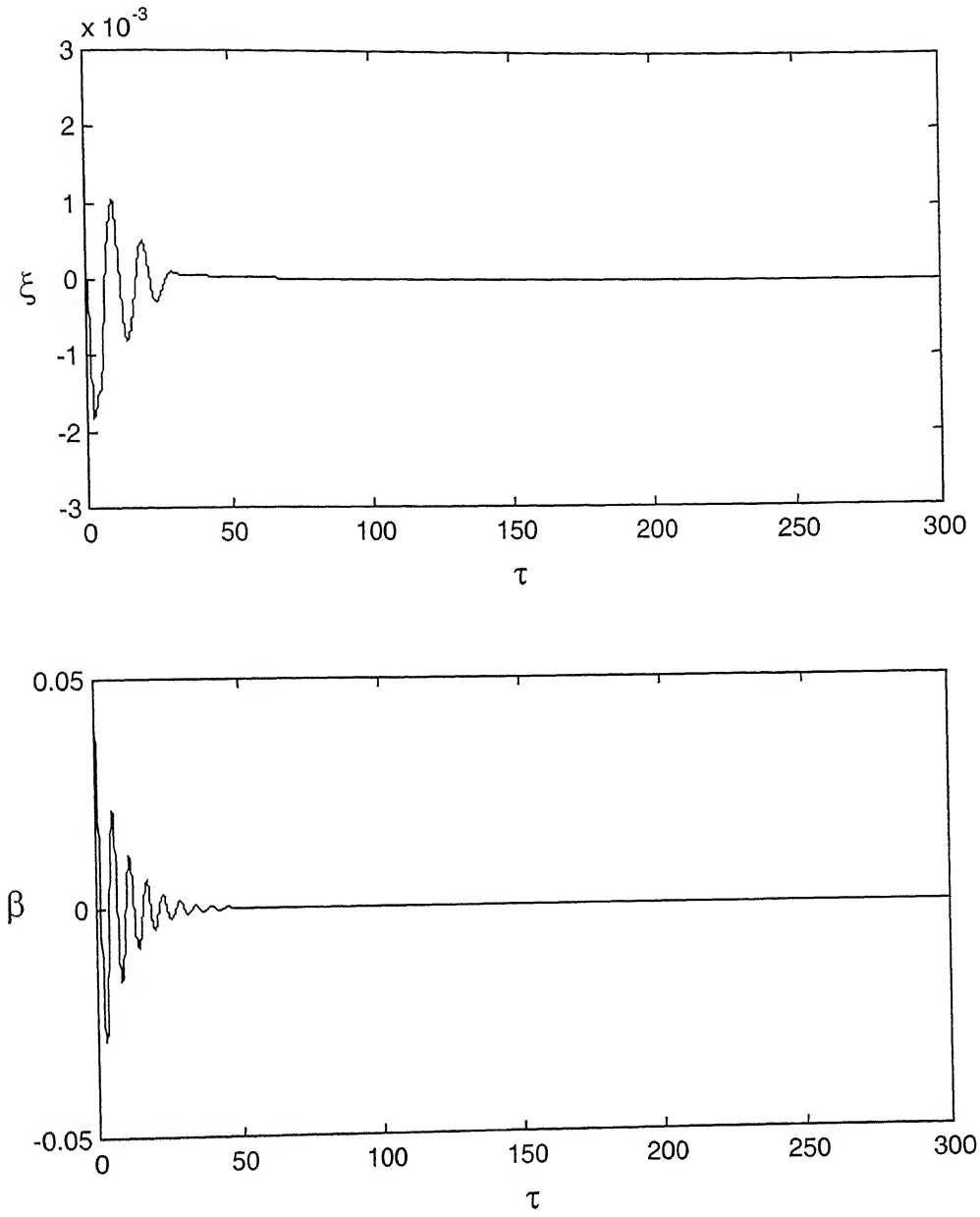

Fig 4.6. Response of Elastomer Model 1 With 10% Flap Damping

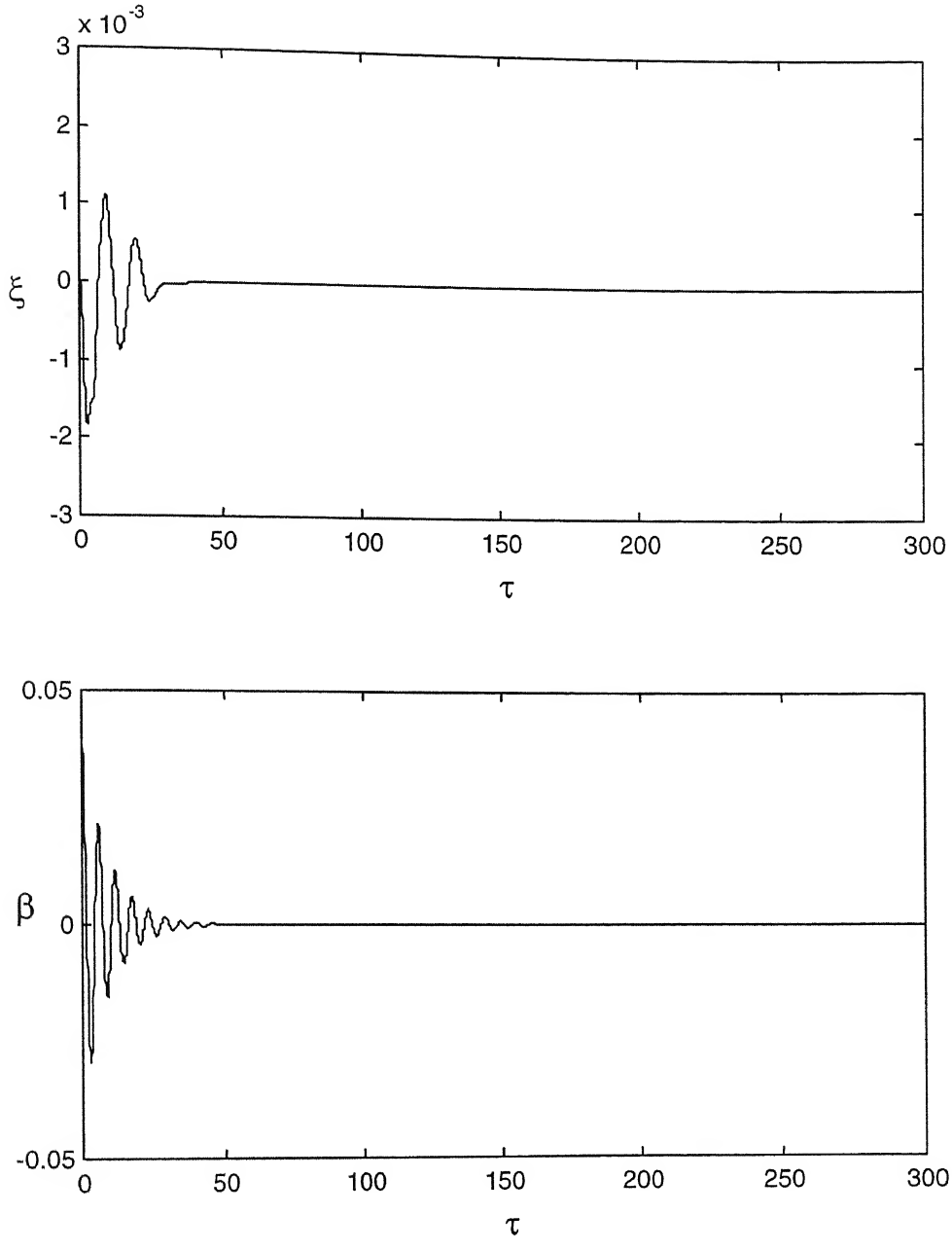

Fig 4.7. Response of Elastomer Model 2 With 10% Flap Damping

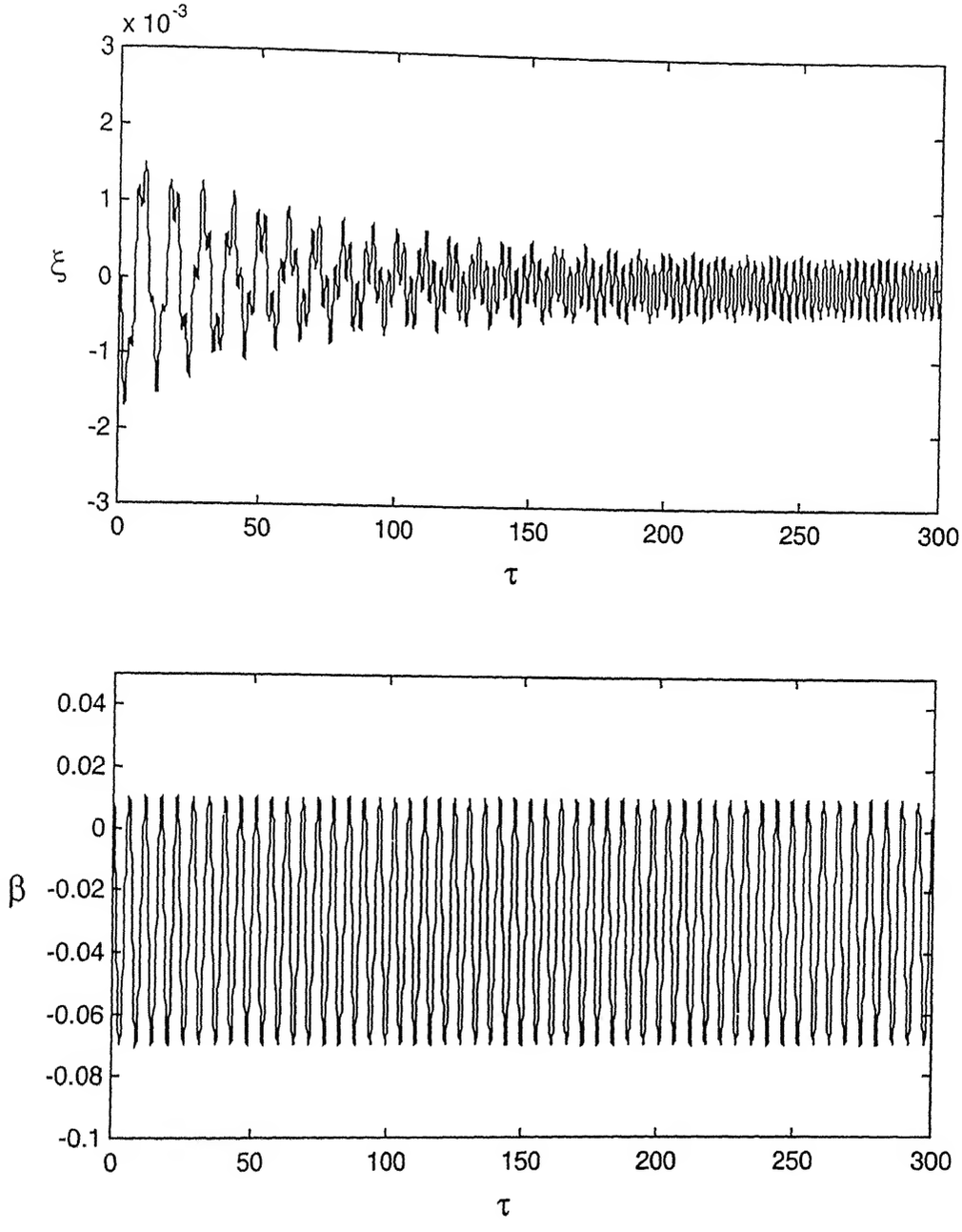

Fig 4.8. Response of Elastomer Model 1 With Precone

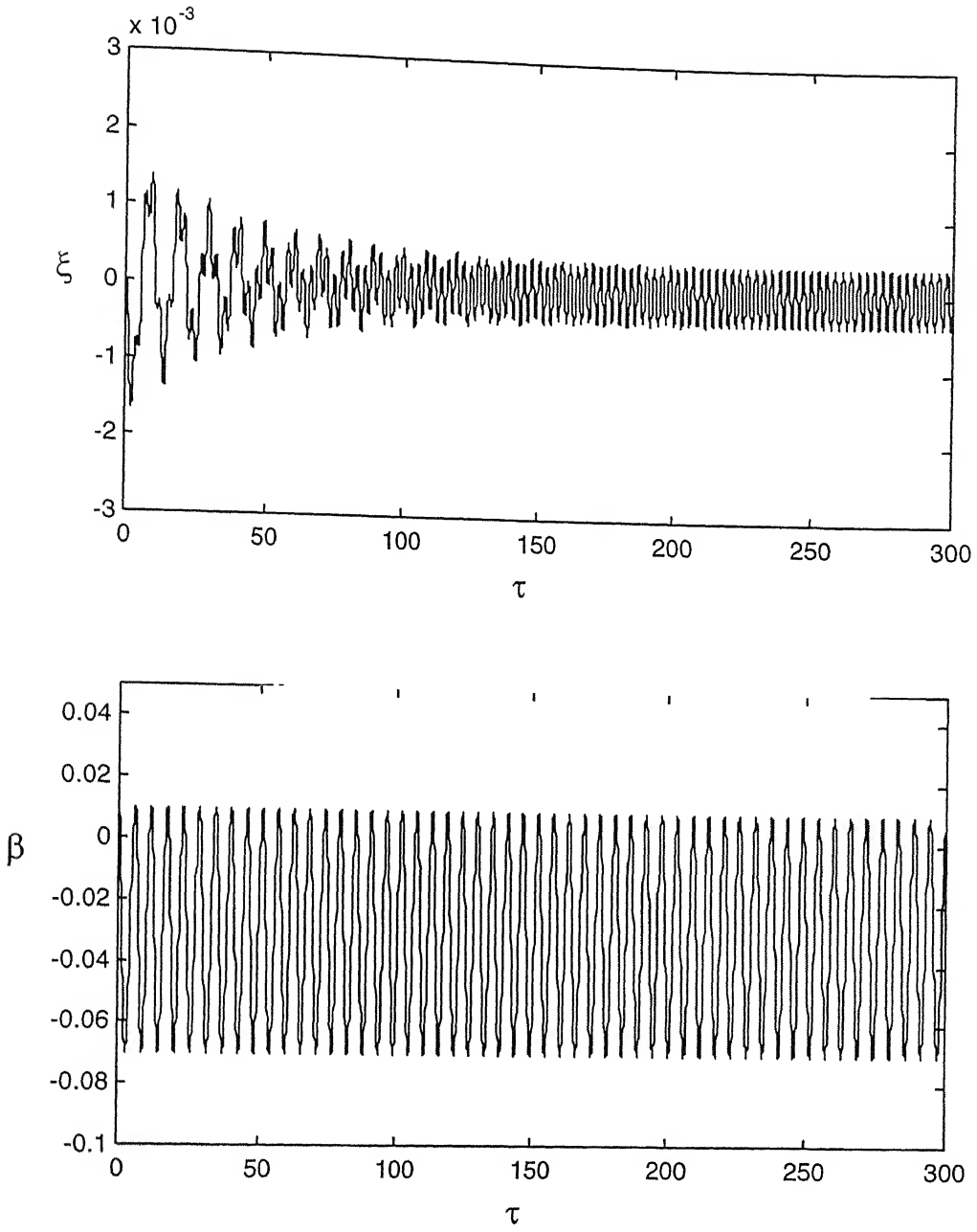

Fig 4.9. Response of Elastomer Model 2 With Precone

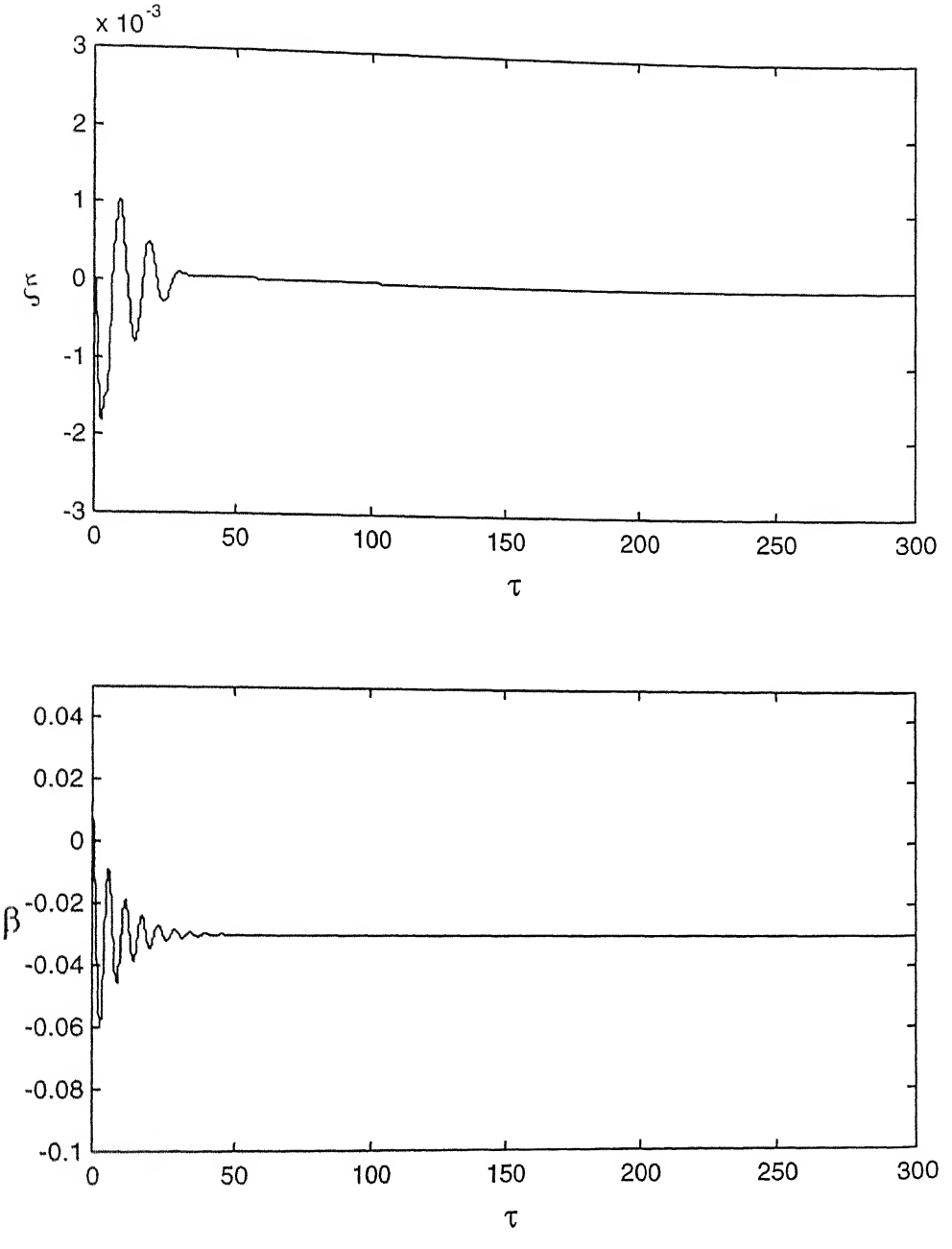

Fig 4.10 Response of Elastomer Model 1 With Precone and 10% Flap Damping

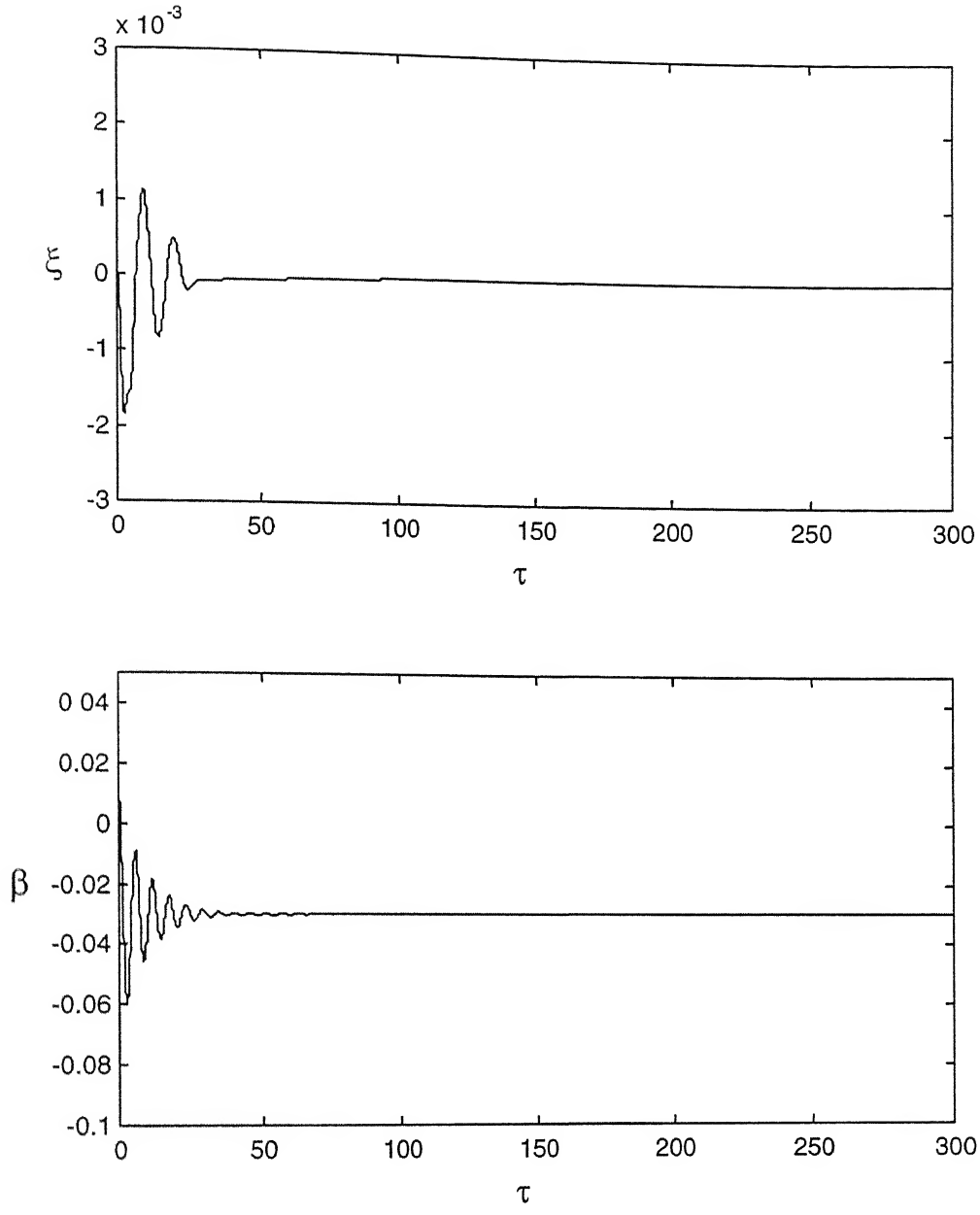

Fig 4.11 Response of Elastomer Model 2 With Precone and 10% Flap Damping

CHAPTER –5

DUAL FREQUENCY ANALYSIS

5.1 INTRODUCTION

To determine the properties of a given damper, lag damper bench tests in the laboratory were conducted using single frequency excitation [8]. But actually the lead lag motion occurs at multiple frequencies simultaneously. The damper properties may not be adequately predicted by a linear superposition of the damper properties at each of the motion frequencies. The highly non-linear characteristics of the elastomeric lag dampers suggest that their properties will also be complex when undergoing a complex motion, and will be different from what is by linear superposition of single frequency test results. The dual frequency motion is of interest because the frequency of the forced response (1/rev) is not the same as the frequency of the potential instability (1^{st} lag mode frequency).

In the present chapter, the analysis of elastomer model will be done taking into consideration two frequencies, the first lag mode frequency, which is 3.3 Hz and the 1/rev of the blade motion, which is 5.4 Hz.

To predict the behavior of elastomer models under the influence of dual frequency excitation, the complex stiffness representation is used. In this method, the in-phase stiffness and quadrature stiffness at different individual frequencies is found out. To find out the in-phase stiffnesses and quadrature stiffnesses at

different frequencies the method of *Fourier transform* is used. If x is an independent variable, and f (x) is its dependent function, then we can write

$$F(\omega) = \int_{-\infty}^{\infty} f(x)\, e^{-i\omega x}\, dx \quad \text{.......... ....(5.1)}$$

Where, $F(\omega)$ is the Fourier transform of $f(x)$, and ω represents an angular frequency.

5.2 METHOD OF DUAL FREQUENCY ANALYSIS

An elastomer lag damper can be characterized in terms of complex damper stiffness K^* as the in-phase or storage stiffness K' and the quadrature or loss stiffness K'', so that

$$K^* = K' + iK'' = K'(1 + i\eta) \quad \text{..............................(5.2)}$$

Where η is the loss factor of the system and is defined as

$$\eta = K''/K'.$$

The quadrature stiffness of the damper is related to the equivalent viscous damping in a way by

$$C_{eq} = \frac{K''}{\omega} \quad \text{..(5.3)}$$

The differential equation of motion for an elastomer Model 1 under the influence of two harmonic forces is given as

$$K_1 x - K_3 x^3 + K_5 x^5 - K_7 x^7 + F \operatorname{sgn}|\dot{x}| + \frac{h}{\omega}\dot{x} = F(t) \quad \text{...............................(5.4)}$$

Where F (t) is exciting force and is given as

$$F(t) = F_1 \cos \omega_1 t + F_2 \cos \omega_2 t$$

Where ω_1 and ω_2 correspond to 3.3 Hz and 5.4 Hz

Let, the solution of this equation is given as

$$x(t) = \mathrm{Re}\,(X e^{i\omega t})$$

Or,

$$x(t) = \mathrm{Re}\,[(X_c + i X_s) e^{i\omega t}]\ ;$$

$$= X_c \cos \omega t - X_s \sin \omega t \quad \text{.....(5.5)}$$

Now x (t) can be assumed to be composed of responses of different amplitudes at different frequencies i.e.

$$x(t) = \sum_{i=1}^{\infty} X_{ci} \cos \omega_i t - X_{si} \sin \omega_i t \quad \text{.....(5.6)}$$

Here X_{ci} and X_{si} are the cosine and sine components of the $x(t)$ at the frequency ω_i. Also the exciting force $F(t)$ can be assumed to be composed of components of exciting forces at different frequencies i.e.

$$F(t) = \sum_{i=1}^{\infty} F_{ci} \cos \omega_i t - F_{si} \sin \omega_i t \quad \text{.....(5.7)}$$

Here F_{ci} and F_{si} are the cosine and sine components of the exciting forces at the frequency ω_i.

Let us take a case at frequency ω_1. The amplitude of exciting force at this frequency is equated to the spring restoring force and damper force at this frequency.

i.e.

$$F(t)_{\omega_i} = K' x(t)_{\omega_i} + \frac{K''}{\omega_i} \dot{x}(t)_{\omega_i} \quad \text{.....(5.8)}$$

Where $F(t)_{\omega_i}$ is the component of exciting force at frequency ω_1 and $x(t)_{\omega_i}$ is the component of response at this frequency K'_{ω_i}; and K''_{ω_i} are in-phase and quadrature stiffnesses at frequency ω_1.

Also, $F(t)_{\omega_i}$ is assumed to be composed of sine and cosine components - $F_{s\omega_i}$ and $F_{c\omega_i}$, respectively, at frequency ω_1. Similarly $x(t)_{\omega_i}$ is made up of its sine and cosine components - $X_{s\omega_i}$, and $X_{c\omega_i}$, respectively. In mathematical form

$$F(t)_{\omega_i} = F_{c\omega_i} \cos \omega_i t - F_{s\omega_i} \sin \omega_i t \quad \text{.....(5.9)}$$

And

$$X(t)_{\omega_i} = X_{c\omega_i} \cos \omega_i t - X_{s\omega_i} \sin \omega_i t \quad \text{.....(5.10)}$$

Putting the values of $X(t)_{\omega_i}$ and $F(t)_{\omega_i}$ from equations (5.9) and (5.10) in equation (5.8)

$$F_{c\omega_i}\cos\omega_i t - F_{s\omega_i}\sin\omega_i t = K'_{\omega_i}\left(X_{c\omega_i}\cos\omega_i t - X_{s\omega_i}\sin\omega_i t\right) + \frac{K''_{\omega_i}}{\omega_i}\left(-X_{c\omega_i}\omega_i\sin\omega_i t - X_{s\omega_i}\omega_i\cos\omega_i t\right) \quad \text{.....(5.11)}$$

Equating sine and cosine terms of both sides of equation (5.11)

$$F_{c\omega_i} = K'_{\omega_i}X_{c\omega_i} - K''_{\omega_i}X_{s\omega_i} \quad \text{.....(5.12)}$$

$$F_{s\omega_i} = K'_{\omega_i}X_{s\omega_i} + K''_{\omega_i}X_{c\omega_i} \quad \text{.....(5.13)}$$

Solving equations (5.12) and (5.13) simultaneously the expressions for in-phase stiffness and quadrature stiffness at frequency ω_i can be obtained as

$$K'_{\omega_i} = \frac{F_{s\omega_i}X_{s\omega_i} + F_{c\omega_i}X_{c\omega_i}}{X^2_{c\omega_i} + X^2_{s\omega_i}} \quad \text{.....(5.14)}$$

And

$$K''_{\omega_i} = \frac{F_{s\omega_i}X_{c\omega_i} - F_{c\omega_i}X_{s\omega_i}}{X^2_{c\omega_i} + X^2_{s\omega_i}} \quad \text{.....(5.15)}$$

Hence, the in-phase and quadrature stiffness at any frequency (ω_i) can be calculated.

5.3 RESULTS AND DISCUSSION

The behavior of elastomer model under dual frequency excitation was studied by many researchers. Felker et al [8] plotted the experimentally obtained in-phase stiffness and quadrature stiffness, which are shown in Fig 5.1 and Fig 5.2, respectively. Wereley et al [17] carried out experiments and plotted the hysteresis loop for the elastomer model under dual frequency excitation, which is shown in Fig. 5.3. In the present section, the results of elastomer damper model are presented and compared with the experimental results.

5.3.1 TIME RESPONSE

The response of the system is obtained by solving equation (5.4). Once again the technique of numerical integration using *fourth order Runge-Kutta* method with a time step of 0.01 is used to get the response. System parameters of Model 1 are taken from Table 2.1. All initial conditions are set to zero. Figure (5.4) shows the response of the system when F_1=1600 N and F_2=0 N i.e., the frequency of exciting force is at 3.3 Hz. Figure (5.5) shows the response of the system when F_1=0 N and F_2=1600 N i.e., the frequency of exciting force is 5.4 Hz. Figure (5.6) represents the response of the system under the influence of dual frequency exciting force. The amplitude of forces applied at 3.3 Hz and 5.4 Hz are F_1 = 800 N and F_2 = 800 N, respectively. From the response of the system it can be observed that the system becomes stationary for a while and then after some time it starts moving (in the single frequency response, the flat peaks and crests denote such situations in Fig. 5.4 and 5.5). This is due to the presence of Coulomb damping force in the model. As soon as the net exciting force (algebraic summation of exciting force and spring restoring force) becomes less than F, the system has zero velocity. The Coulomb damping force will not allow the system to move. The system will remain at that position until the net exciting force becomes less that –F. Afterwards the system will be moving in reverse direction.

5.3.2. FREQUENCY RESPONSE

To get the information of other frequencies present in the response, it is essential to view the frequency-response. The frequency response of the system is obtained by taking *Fast Fourier Transform* of the time responses of the system. The number of data points taken is 1024. Figure (5.7) shows the FFT of the system response when F_1=1600 N and F_2 =0 N i.e., the exciting force is at 3.3 Hz. In the response so many peaks at other frequencies are observed. Apart from 3.3 Hz the other important frequencies are 9.9 Hz, 16.5 Hz, 23.1 Hz, 29.7 Hz, and 36.3 Hz. Figure (5.8) shows the FFT of the response when F_1 =0 N and F_2 =1600 N. The

dominant frequencies apart from 5.4 Hz are 16.2 Hz, 27 Hz, 37.8 Hz and 48.6 Hz. Figure (5.9) shows the response of the system under dual frequency excitation, the amplitudes of exciting forces are 1600 N at 3.3 Hz and 1600 N at 5.4 Hz. Here peaks at following frequencies are observed in the order of decreasing amplitude: 3.3 Hz, 5.4Hz, 1.1Hz, 7.5Hz, 12.0Hz, 9.9Hz, 14.1Hz, 22.8Hz, 0.9Hz, 20.7Hz, 3.0Hz, 9.6Hz, 5.6Hz, 5.1Hz, 3.6Hz, 11.7Hz, 18.5Hz, 18.3Hz, 24.9Hz, and 16.2Hz.

5.4.3. HYSTERESIS CURVE

For analysing the effect of dual frequency on hysteresis curve, hysteresis curves are plotted for different cases keeping the amplitude of one exciting force (at 3.3 Hz) constant and then varying the amplitude of the other exciting force (at 5.4 Hz). Figure (5.10) shows hysteresis curve when F_1=1600 N F2=0 N i.e., for a single frequency excitation (at 3.3 Hz). For single frequency excitation a single loop is observed. Figure (5.11) shows the hysteresis curve when F_1 =1600 N and F_2 =400 N and Fig (5.12) shows for the case when F_1=1600 N and F_2 =800 N. It can be observed that, in case of single frequency excitation the hysteresis curve consists of single loop, but for dual frequency excitation multiple loops are observed. This is an important characteristic of elastomer damper model with non-linearities. These trends match with the experimental results of Wereley et al. [17], which is shown in Fig. (5.3).

5.3.4. IN-PHASE AND QUADRATURE STIFFNESS

The most important thing in the analysis of dual frequency excitation is to get the in-phase stiffness and the quadrature stiffness. The in-phase and quadrature stiffness are obtained from equations (5.14) and (5.15). Figure (5.13) shows the in phase stiffness at 3.3 Hz keeping F_1 constant and varying F_2. There are six different curves in Fig. (5.13) for different F_1 (0N, 400N, 800N, 1200N, 1600N, and 2000N). The first curve is for F_1= 0N. This is obtained by varying F_2 form 400 to 2000 N. For each value of F_2 the FFT of response is obtained (with F_1= 0

N). From the FFT of response the values of $X_{c3\,3}$ and $X_{s3\,3}$ are obtained. The values of $F_{c3\,3}$ and $F_{s3\,3}$ can be obtained from the FFT of the exciting force. Putting these values in equation (5.14) the in-phase stiffness and in equation (5.15) the quadrature stiffness are obtained for this pair of F_1 and F_2. Now changing F_2 (400N, 800N, 1200N, 1600N, 2000N) for F_1=0 N, we get as many as six points. These six points generate the first curve for F_1 =0 N. In this way one curve for different F_1 is obtained. Similarly taking different F_1 (400N, 800N, 1200N, 1600N, and 2000N) five more curves are obtained. The quadrature stiffness for the case is shown in Fig. 5.14. Now, keeping F_2 constant and varying F_1, the in-phase stiffness at 3.3 Hz is obtained (Figure 5.15). In a similar fashion we get two more curves for in-phase stiffness corresponding to 5.4 Hz. In this way the following matrix of plots are obtained for in-phase stiffness and quadrature stiffness.

a) In phase stiffness at 3.3 Hz keeping F_1 constant and varying F_2 (Fig. 5.13)
b) Quadrature stiffness at 3.3 Hz keeping F_1 constant and varying F_2 (Fig. 5.14)
c) In phase stiffness at 3.3 Hz keeping F_2 constant and varying F_1 (Fig. 5.15)
d) Quadrature stiffness at 3.3 Hz keeping F_2 constant and varying F_1 (Fig. 5.16)
e) In phase stiffness at 5.4 Hz keeping F_2 constant and varying F_1 (Fig. 5.17)
f) Quadrature stiffness at 5.4 Hz keeping F_2 constant and varying F_1 (Fig. 5.18)
g) In phase stiffness at 5.4 Hz keeping F_1 constant and varying F_2 (Fig. 5.19)
h) Quadrature stiffness at 5.4 Hz keeping F_1 constant and varying F_2 (Fig. 5.20)

Figures 5.1 and 5.2 shows the plot for in-phase stiffness and quadrature stiffness as obtained by Felker et al. [8]. Comparing Figs. 5.13 to 5.20 with that of Fig. (5.1) and Fig. 5.2 it is observed that the elstomer model under consideration is unable to predict the experimental results. Therefore it can be concluded that the models need refinement through further research.

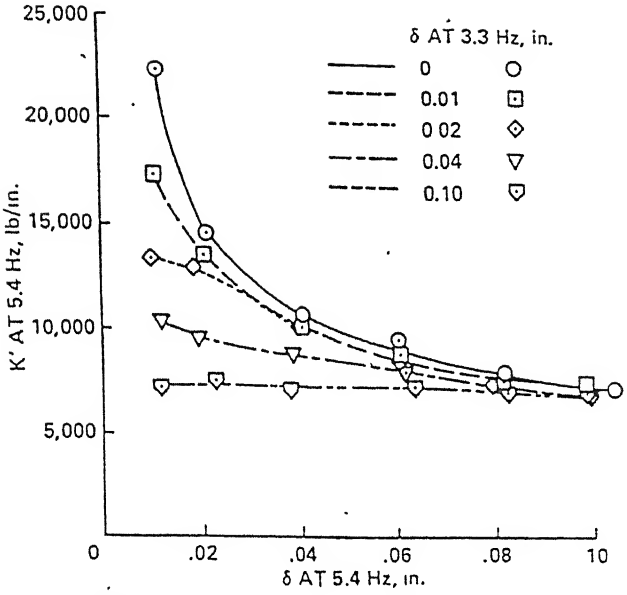

Bell 412 Damper Spring Rate at 5.4 Hz with Dual-Frequency Motion.

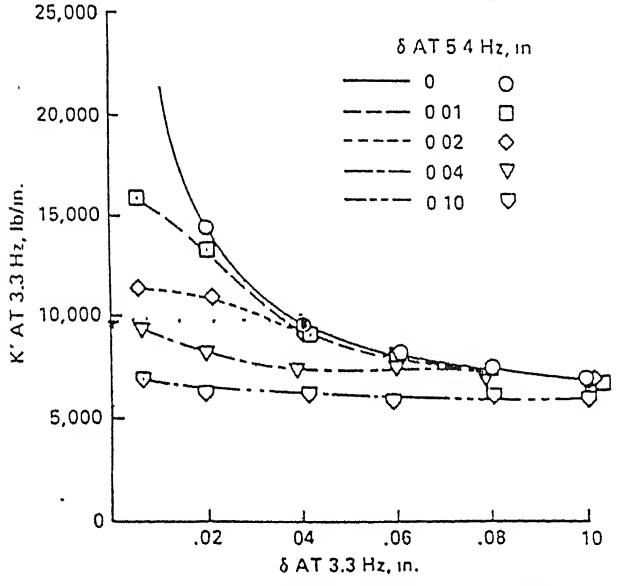

Bell 412 Damper Spring Rate at 3.3 Hz with Dual-Frequency Motion.

Figure 5.1 In-phase stiffness for dual frequency excitation from Ref. [8]

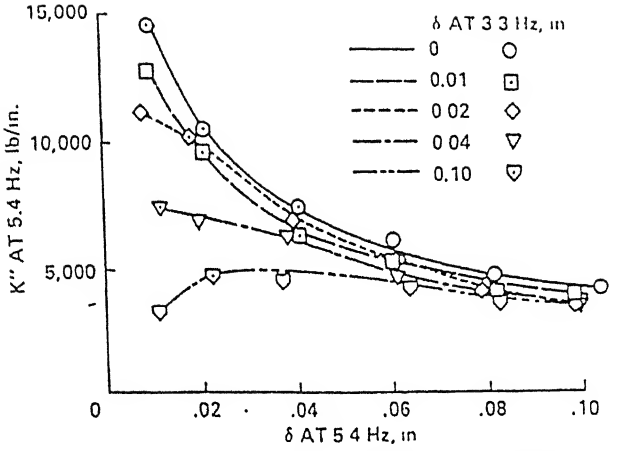

Bell 412 Damper Damping at 5.4 Hz with Dual-Frequency Motion.

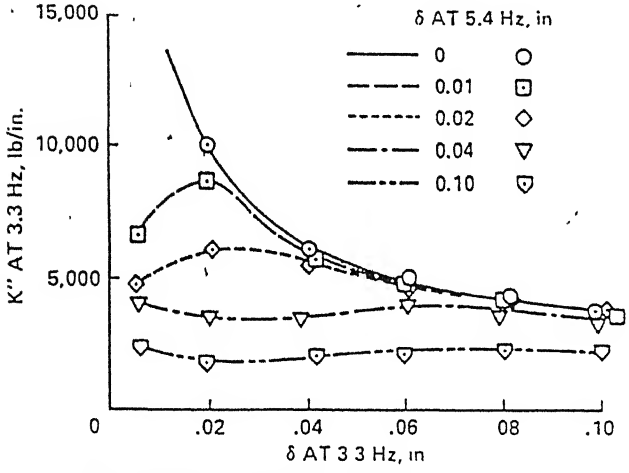

Bell 412 Damper Damping at 3.3 Hz with Dual-Frequency Motion.

Figure 5.2 Quadrature stiffness for dual frequency excitation from Ref. [8]

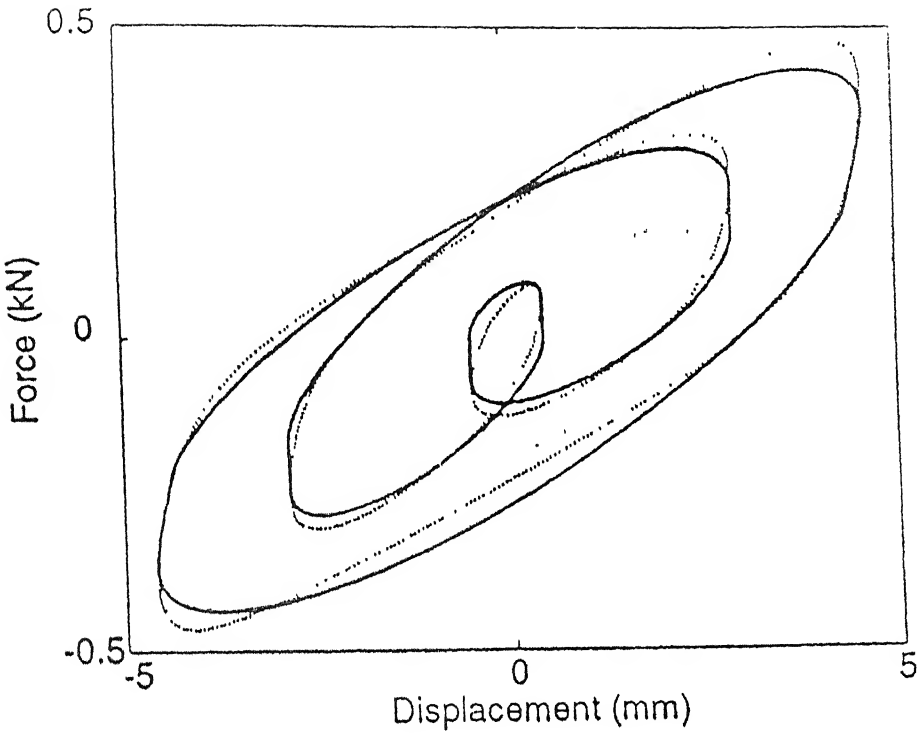

Figure 5.3 Hysteresis loop for dual frequency excitation as obtained by Wereley et al. [17]

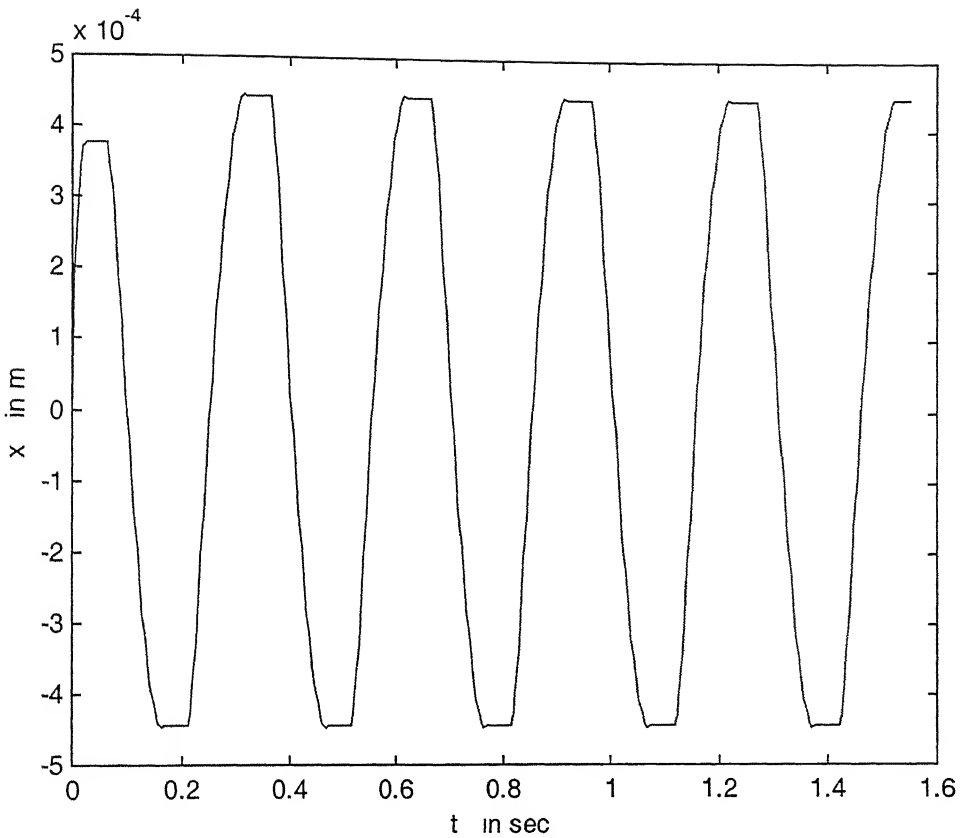

Figure 5.4 Response of the system when F1 =1600 N and F2= 0 N

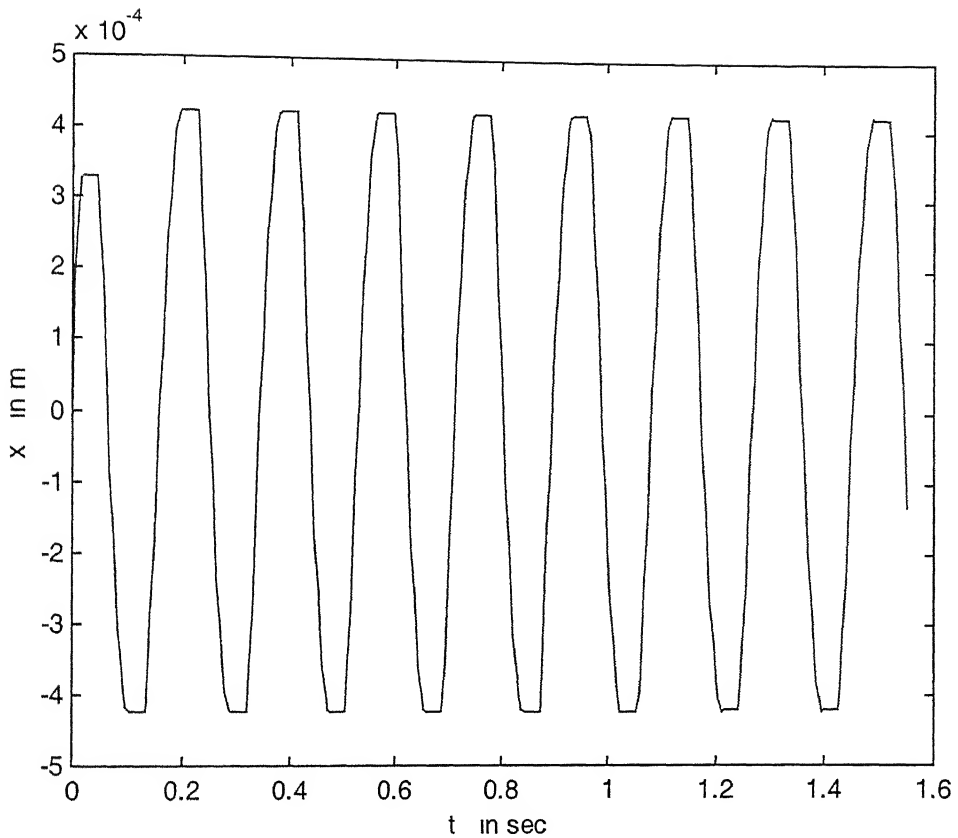

Figure 5.5 Response of the system when F1 = 0 and F2= 1600 N

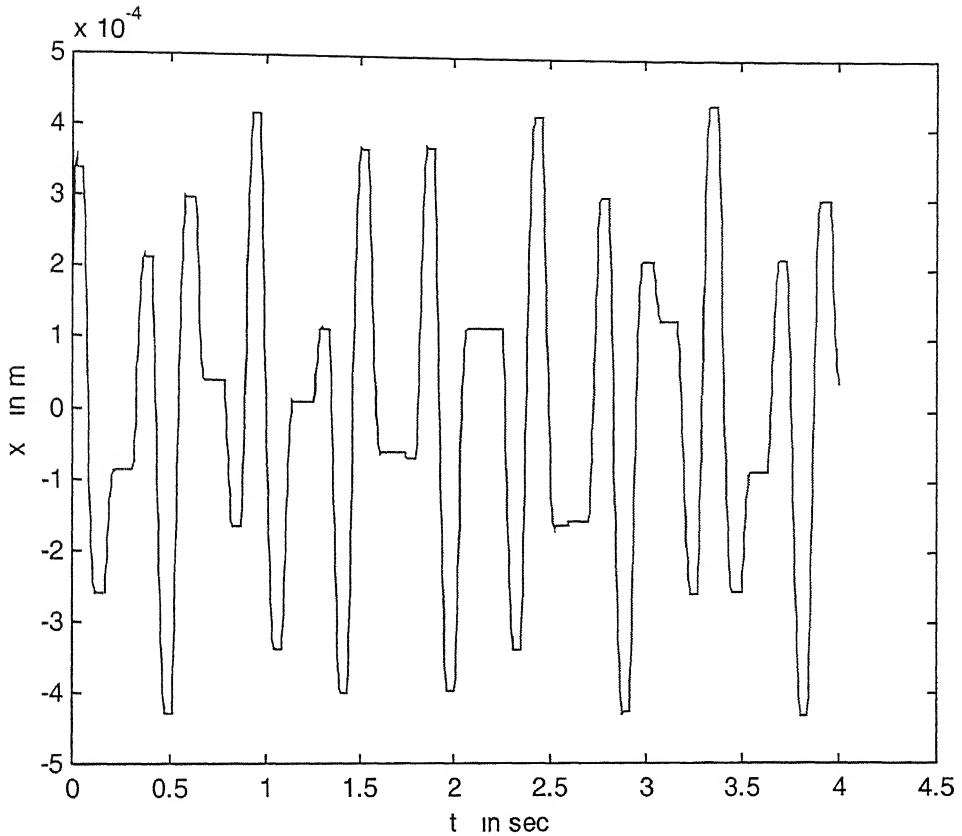

Figure 5.6 Response of the system when F1 = 800 N and F2= 800 N

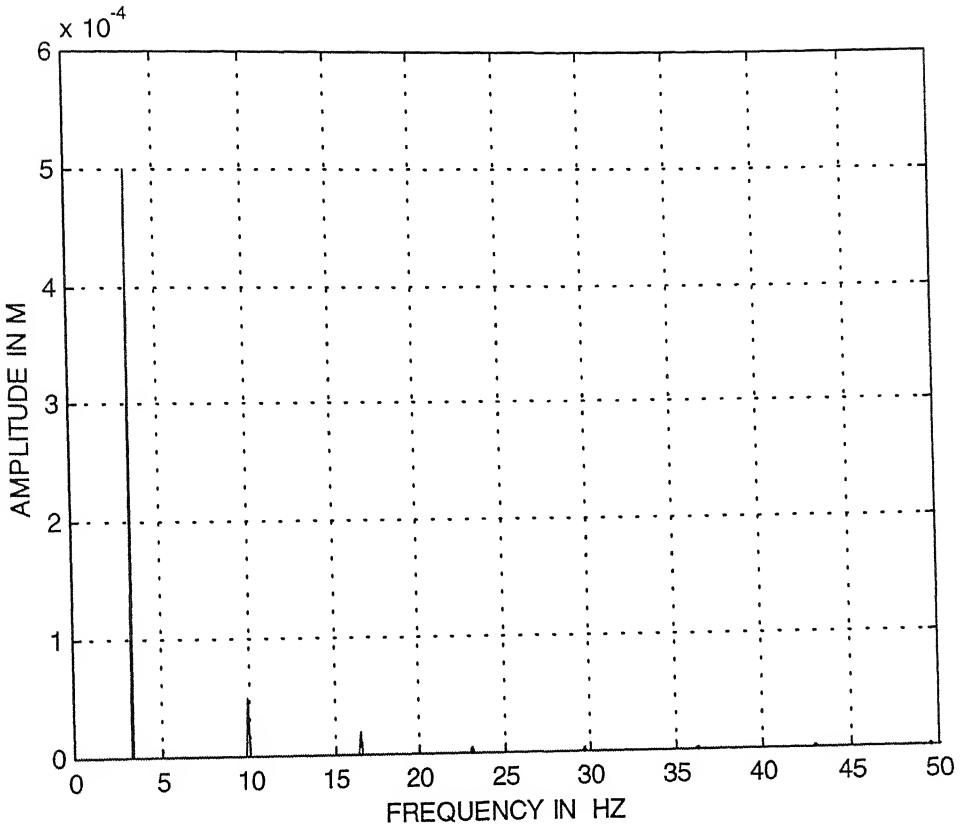

Figure 5.7 FFT of response when F1 = 1600 N and F2 = 0 N

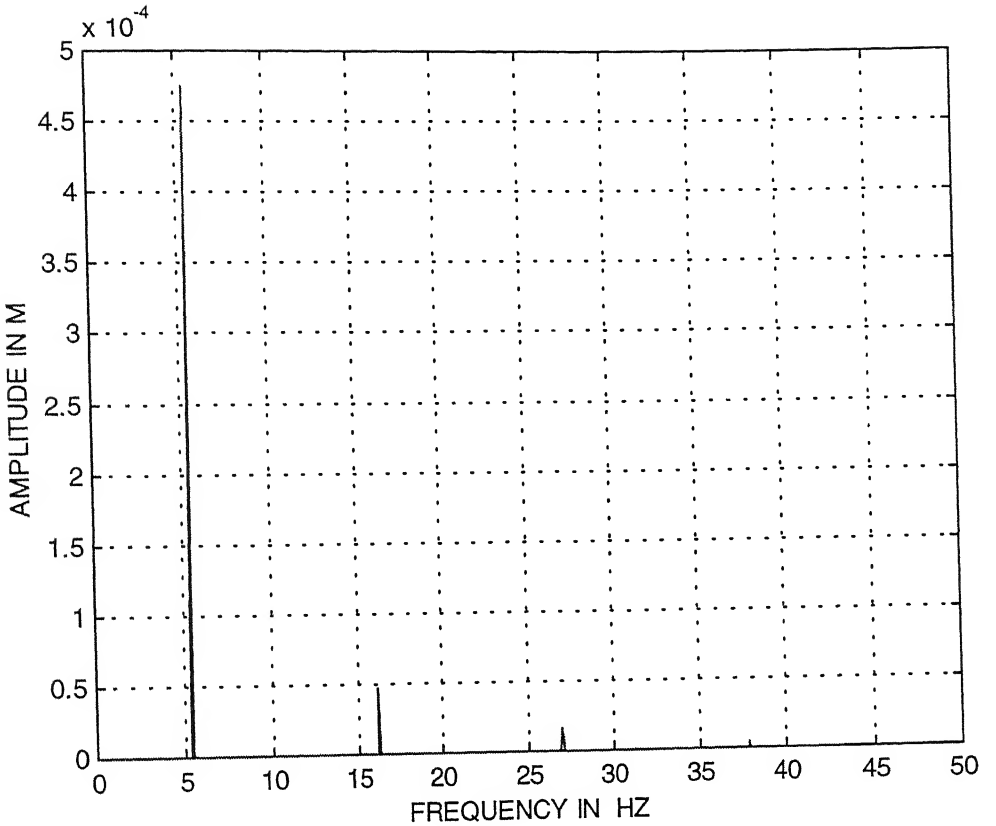

Figure 5.8 FFT of response when F1 = 0 N and F2 = 1600 N

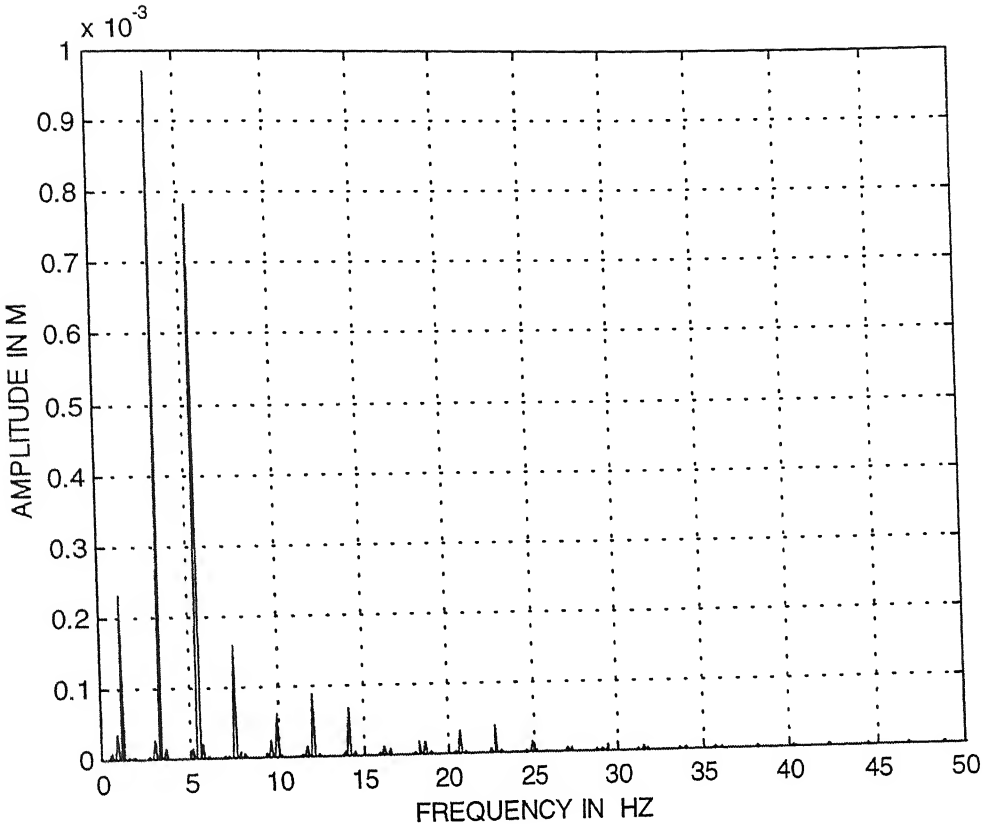

Figure 5.9 FFT of response when F1 =1600 N and F2 = 1600 N

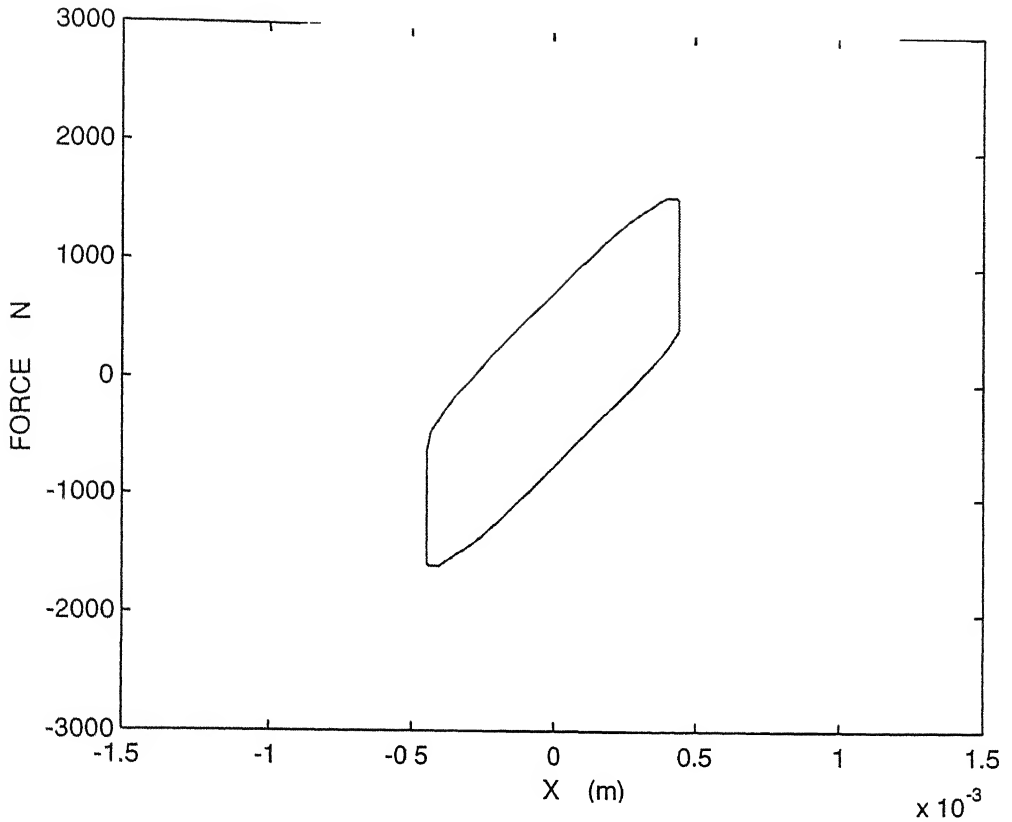

Figure 5.10 Hysteresis Loop When F_1=1600 N and F_2=0 N
(i.e. For Single Frequency Excitation)

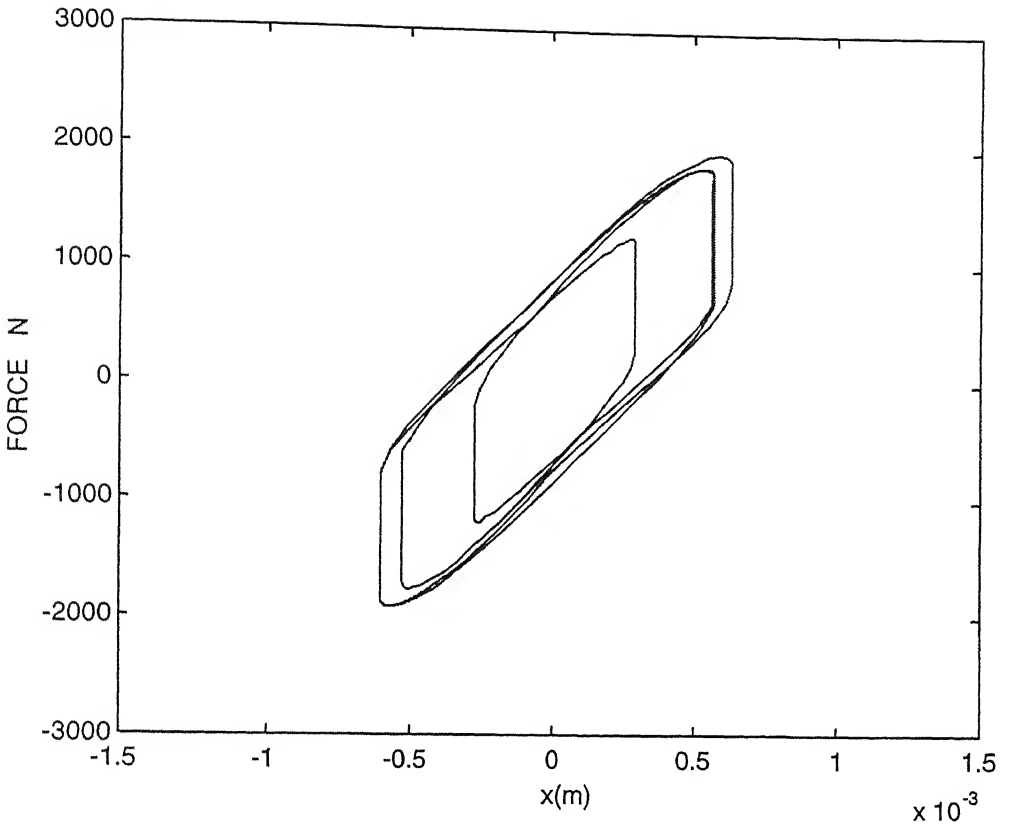

Figure 5.11 Hysteresis Loop When F_1=1600 N and F_2 =400 N

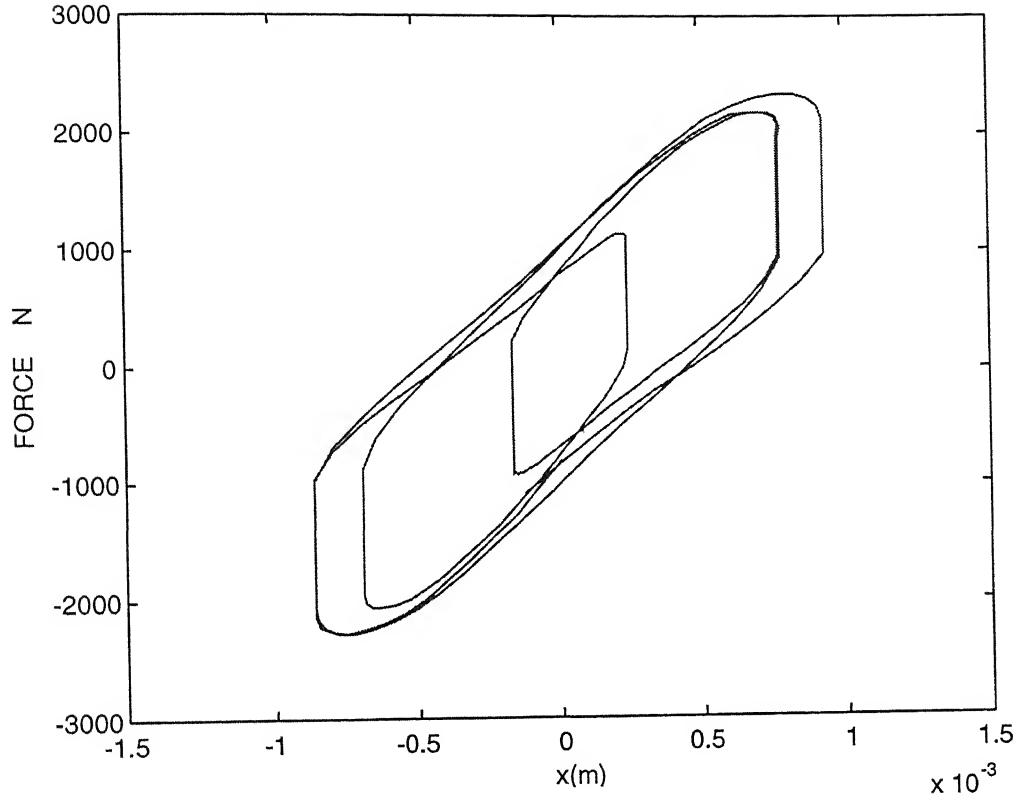

Figure 5.12 Hysteresis Loop When F_1 =1600 N and F_2 =800 N

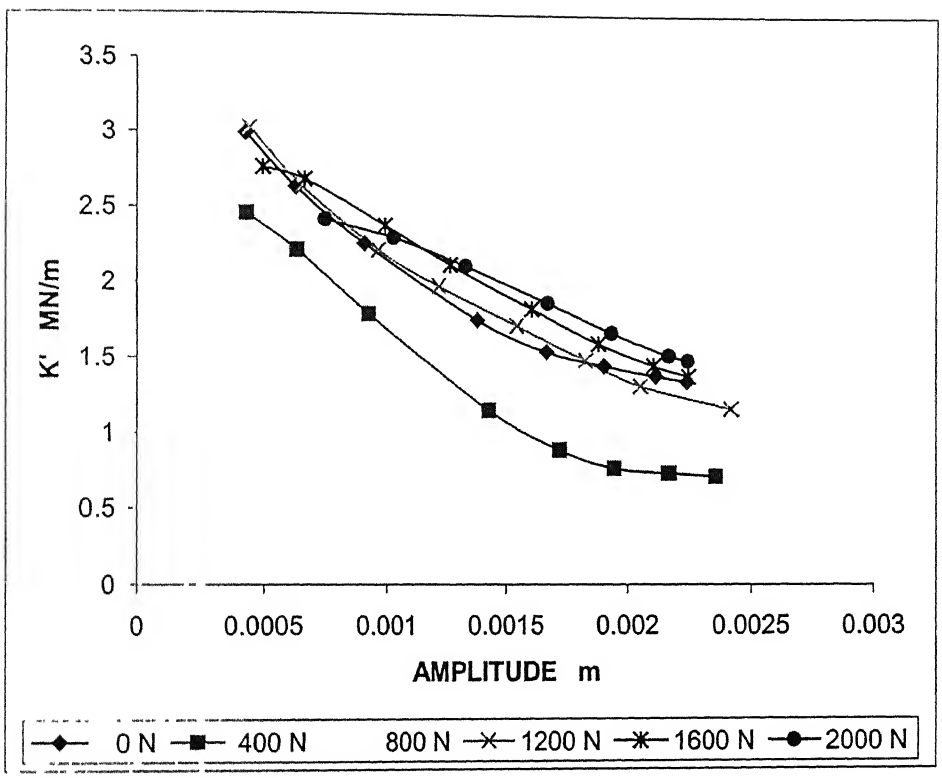

Figure 5.13 In phase stiffness (K') at 3.3 Hz keeping F_1 constant and varying F_2

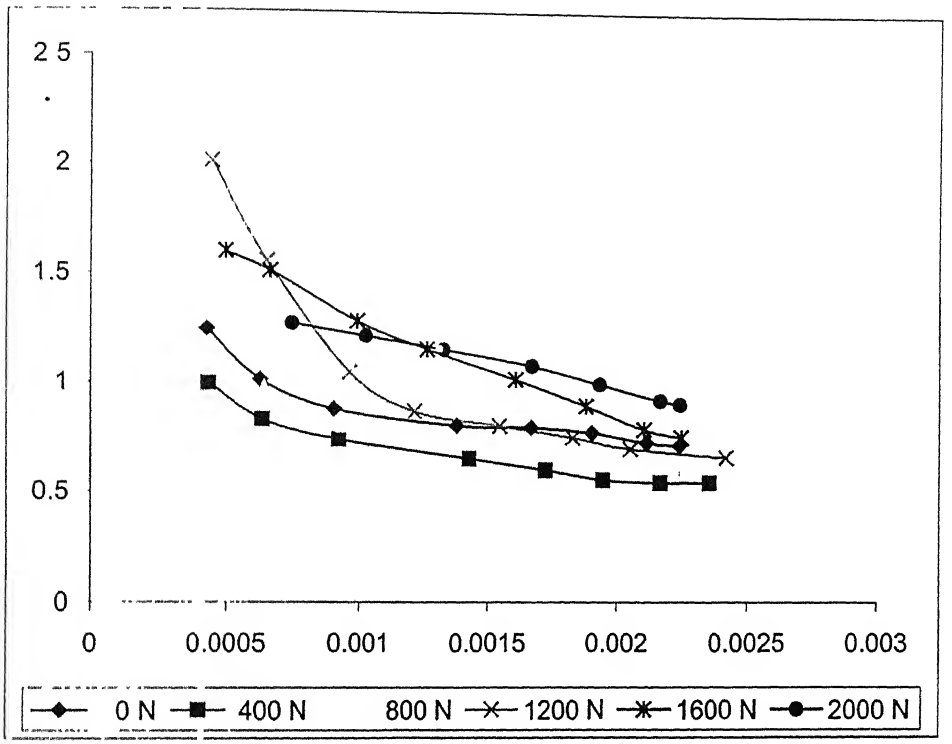

Figure 5.14 Quadrature stiffness (K'') at 3.3 Hz keeping F_1 constant and varying F_2

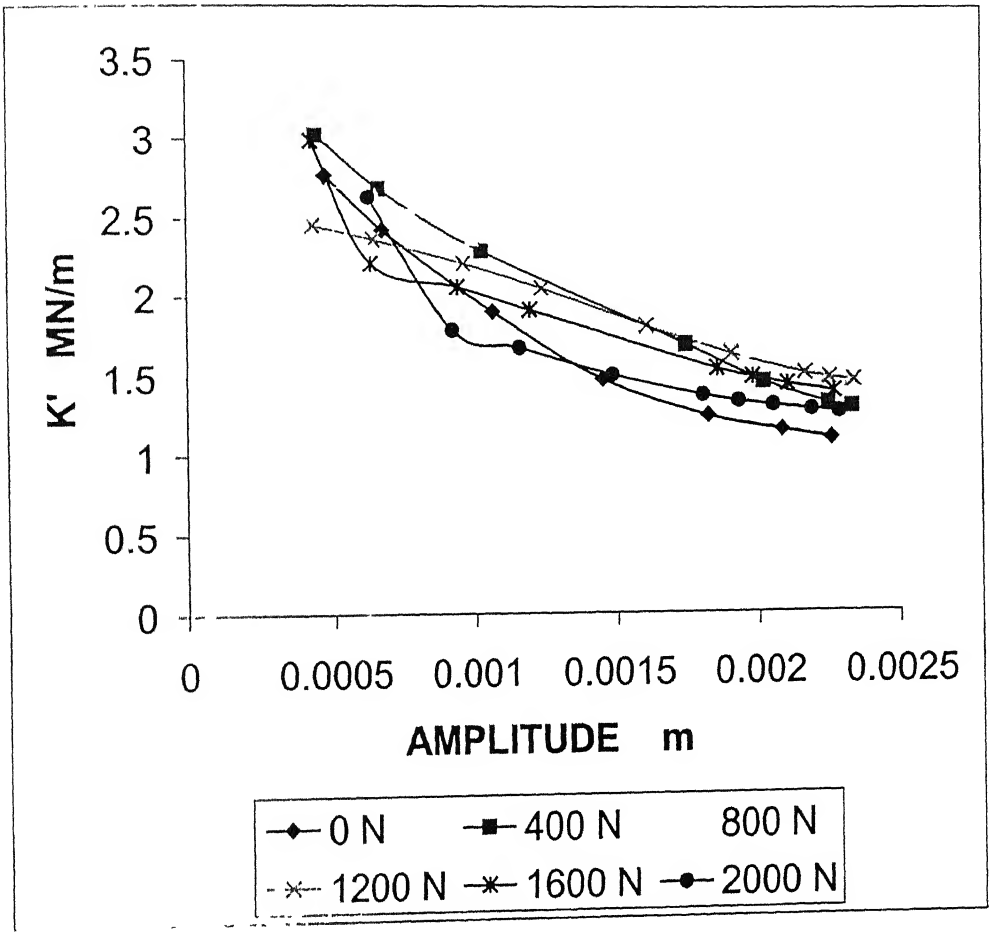

Figure 5.15. In phase stiffness (K') at 3.3 Hz keeping F_2 constant and varying F_1

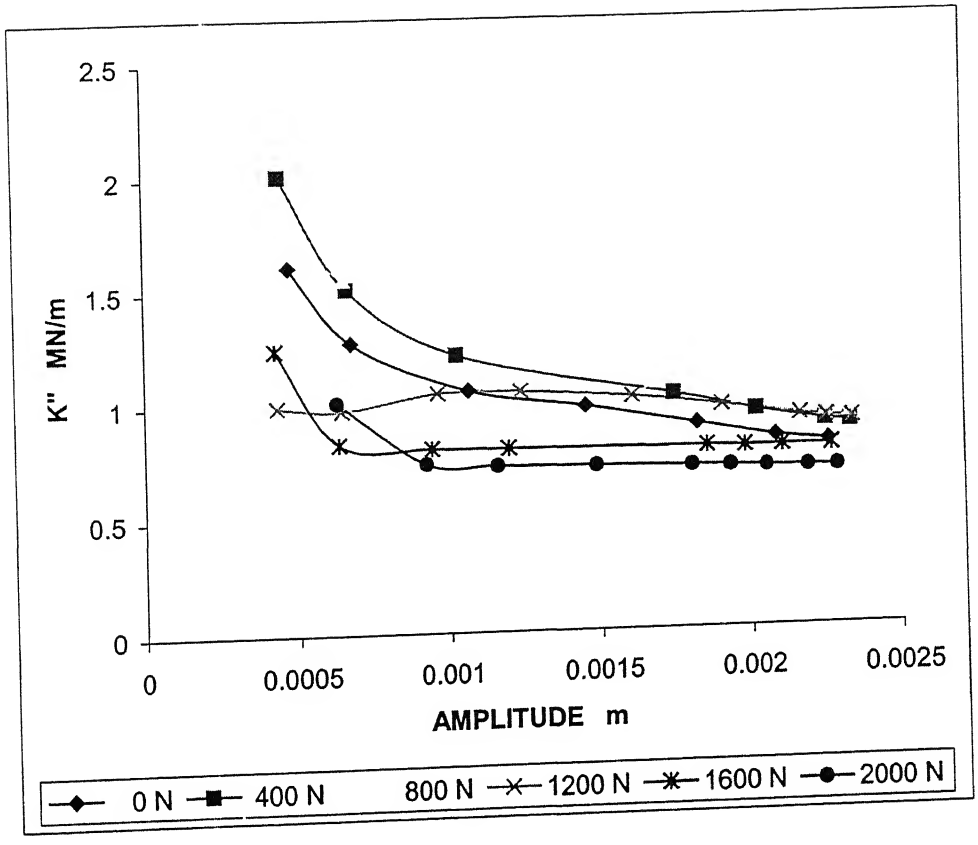

Figure 5.16 Quadrature stiffness (K'') at 3.3 Hz keeping F_2 constant and varying F_1

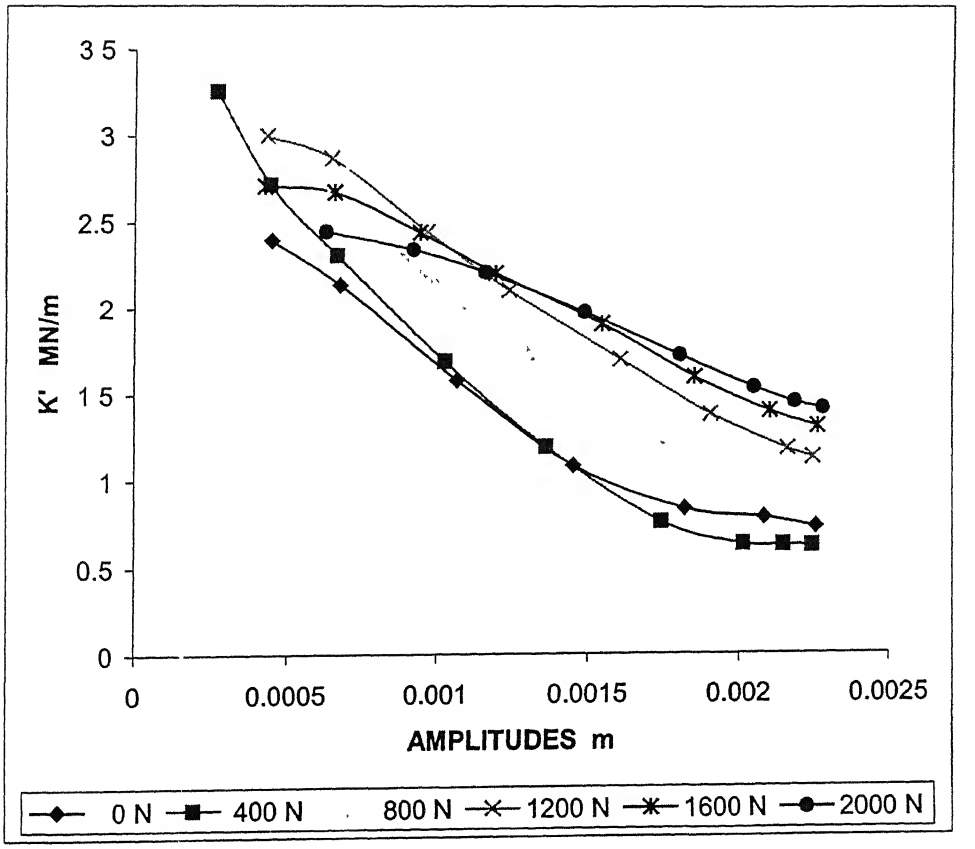

Figure 5.17 In phase stiffness (K') at 5.4 Hz keeping F_2 constant and varying F_1

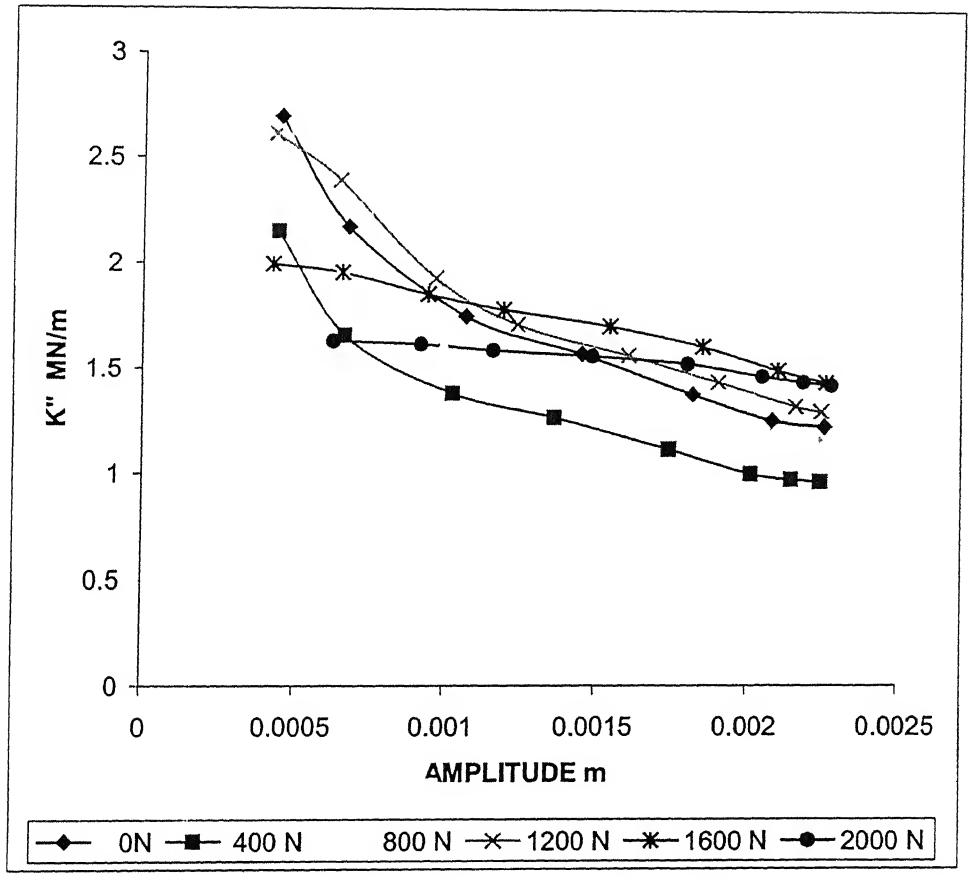

Figure 5.18 Quadrature stiffness (K'') at 5.4 Hz keeping F_2 constant and varying F_1

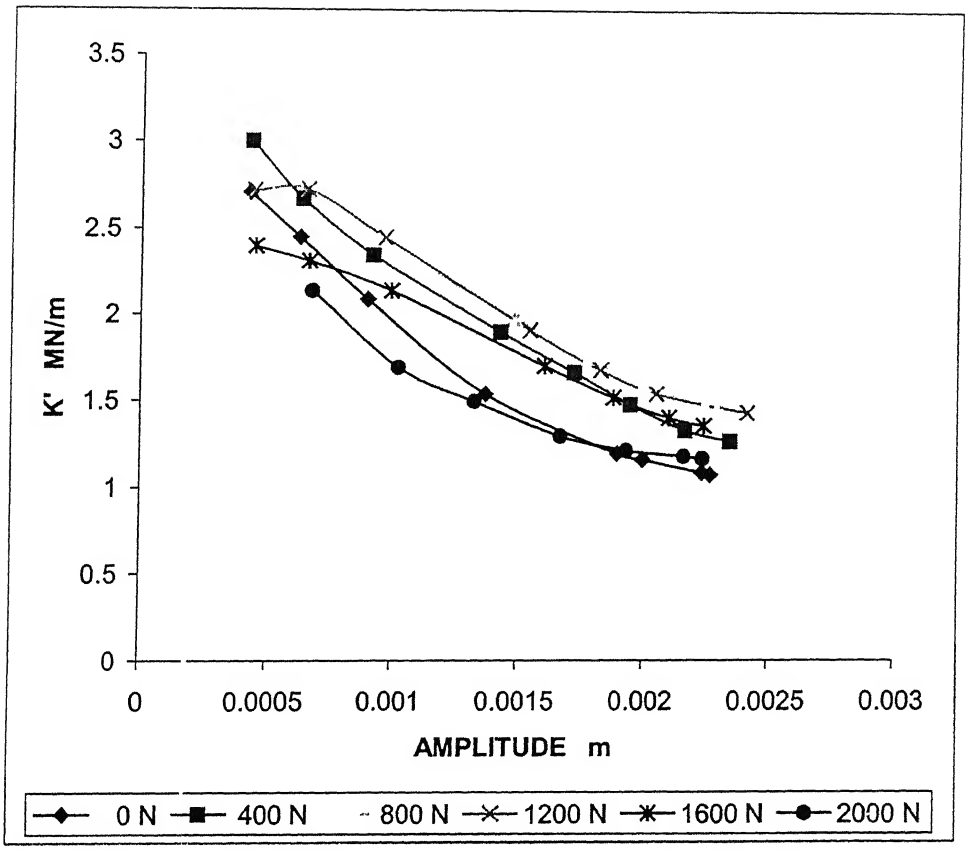

Figure 5.19 In phase stiffness (K') at 5.4 Hz keeping F_1 constant and varying F_2

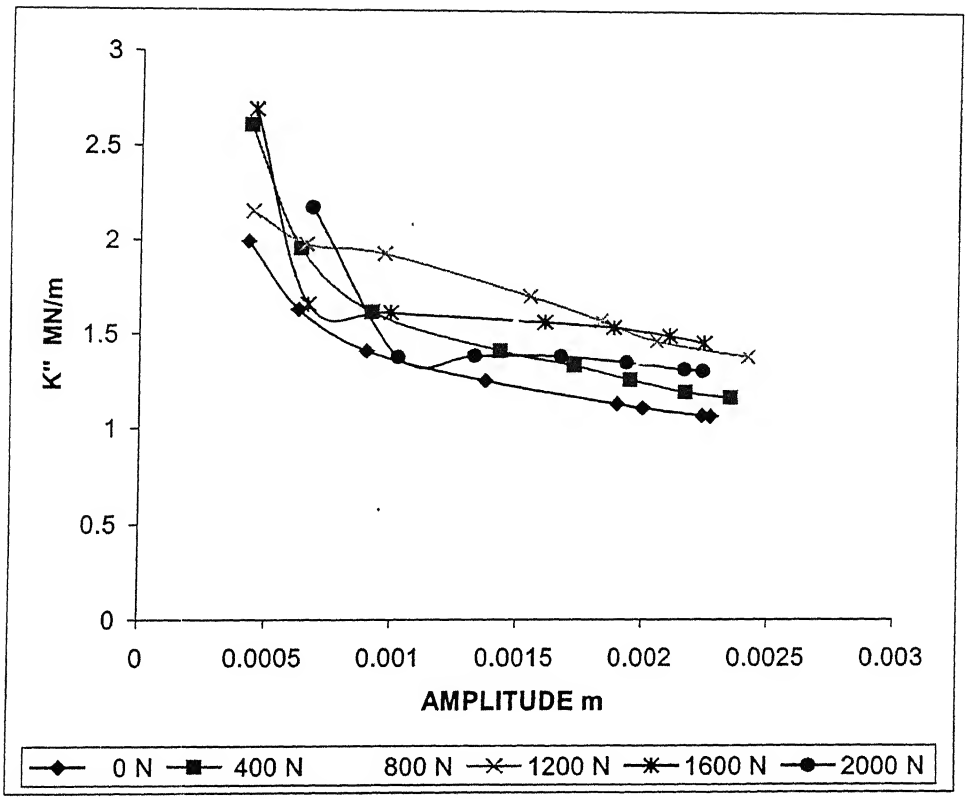

Figure 5.20 Quadrature stiffness (K'') at 5.4Hz keeping F_1 constant and varying F_2

CHAPTER-6

CONCLUSIONS

In the present work, the effect of modelling of elastomers on various dynamical systems of increasing complexity has been studied with respect to two elastomer models. First model is a parallel combination of a non-linear spring, a Coulomb damper and a hysteretic damping element. Second model consists of a non-linear spring, a Coulomb damping element, and Rayleigh type hysteretic damping element. The major conclusions of the present study are summerised below.

1. From the plot of non-linear spring force vs. amplitude, it was observed that the spring force becomes negative as soon as the amplitude of motion becomes greater than 0.0026m. Therefore in all calculations, the amplitude of motion has been restricted to less than 0.0026m.
2. For the uncoupled lag mode motion, the system is stable and oscillations damp out for both the models. Also, both models predict identical behavior and there is no evidence of the occurrence of limit cycle oscillations.
3. The effect of flap lag coupling is of one-way type. There is no transfer of energy from lag mode to flap mode, but the reverse is not true. The coupled flap lag mode exhibits limit cycle oscillation in lag mode irrespective of the elastomer models. The flap mode oscillates with constant amplitude. Also inserting a very small amount of damping in the flap mode, the motion ceases for both the models.

4. In the case of dual frequency excitation, the system becomes stationary for a while due to the presence of Coulomb damping in the models. The frequency response exhibits presence of many frequencies other than those excited. The hysteresis curve in case of single frequency excitation consists of a single loop only, while in case of dual frequency excitation it consists of multiple loops. The plots for in-phase and quadrature stiffness for both the models do not agree with the experimental results found in the open literature. Therefore both models need further refinement.

REFERENCES

1. Fung, Y. C., *Foundation of Solid Mechanics*, Prentice-Hall, Englewood Cliffs, NJ, 1965, pp. 412 –420
2. Glockner, P.G., and Szyszkowski, W , "An Engineering Multiaxial Constitutive Model for Non-linear Time Dependent Materials," *Int J Solid Structures*, Vol. 26, No. 1, 1990, pp. 73-82.
3. Szyszkowski, W. and Glockner, P.G, "A Non-linear Constitutive Model for Ice," *Int J Solid Structures*, Vol. 21, No. 3, 1985, p.p. 307-321.
4. Polter, J. L., McGuire, D. P., and Brubaker, E. L, "Elastomers + Fluids+ Electronics=Improved Comfort and Reliability for Aircrafts," *Proceedings of the International Exhibition Cum seminar on Helicopter Development and Utilisation in South Asia-pacific*, Banglore, India, Oct.1995, pp. 6.3.1-6.3.19
5. McGuire, D. P., " The Application of Elastomeric Lead-lag Dampers to Helicopter Rotors," Lord library No. LL2133.
6. Housmann, G , and Gergely, P., "Approximate Methods for Thermoviscoelastic Characterization and Analysis of Elastomeric Lead-lag Dampers," *Eighteenth European Rotorcraft Forum*, Avignon, France, Sept 1992, pp. 88.1-88.17.
7. Housmann, G., "Structural analysis and Design Consideration of Elastomeric Dampers with Viscoelastic Material Behavior," *Twelft European Rotorcraft Forum,* Garmisch-Partekirchon, Germany, Sept 1986, pp 70.1-70.26
8. Felker, F., lau, B., McLaughlin, S., and Johnson, W.; " Non-linear Behavior of an Elastomeric Lag Damper Undergoing Dual frequency Motion and its Effect on Rotor Dynamics," *Journal of the American Helicopter Society*, Vol. 34, No. 4, 1987, pp. 45-53.

9. Gandhi, F., and Chopra, I., "Analysis of Bearingless Main Rotordynamics with the Inclusion of an Improved Time Domain Non-linear Elastomeric Damper Model," *Journal of the American Helicopter Society*, Vol. 41, No. 3, 1996, pp. 267-277.

10. Ormiston, R. A., Saberi, H., and Anastassiades, T., "Application of 2G CHAS to the Investigation of Aeromechanical Stability of Hingeless Rotor Helicopter", *51st Forum of the American Helicopter Society*, Fort Worth, TX, May 1995, pp.1132-1155.

11. Kunz, D. L., "Influence of Elastomeric Damper Modeling on the Dynamic Response of Helicopter Rotors," *AIAA Journal*, Vol. 35, No. 2, 1997, pp. 349-354.

12. Smith, E. C., Beale M. R., Govindswamy, K., Vascsinec, M. J., and Lesieutre, G. A., "Formulation and Validation of a Finite Element Model for Elastomeric Lag Dampers", *51st Annual Forum of the American Helicopter Society*, Fort Worth, TX, May 1995, pp. 1101-1116.

13. Pohit, G., " Dynamics of a Bearingless Helicopter Rotor Blade with a Nonlinear Elastomeric Constraint", Ph.D. Thesis, Dept. of Mechanical Engineering, Indian Institute Of Technology, Kanpur, India, 1999.

14. Pohit, G., Mallik, A. K., and Venkatesan, C., "Free Out-of-Plane Vibration of Rotating Beam with Non-linear Elastomeric Constraints", *Journal of Sound and Vibration*, Vol. 220, No. 1, 1999, pp. 1-25.

15. Pohit, G., Mallik, A. K., and Venkatesan, C., "Influence of Non-linear Elastomer on Isolated Lag Dynamics and Rotor/Fuselag Aeromechanical Instability", *AIAA Paper*, No. 1691, April 2000.

16. Pohit, G., Mallik, A. K., and Venkatesan, C., "Elastomeric Damper Model and Limit Cycle Oscillation in Bearingless Helicopter Blade", *Journal of Aircraft*, Vol. 37, No. 5, 2000, pp. 923-926

17. Wereley, N. M., Snyder R., Krishnan R., and Sieg T., " Helicopter Damping", *Encyclopedia of Vibration*, Edited by Ewins, D., and Rao, S. S., Academic Press 2001, pp. 629-642

18. Venkatesan, C., "Nonlinear Modeling of Elastomeric Damper and its Influence on Bearingless Rotor Blade Dynamics," Paper presented at *Aero-India 2001*, 7-9 February 2001, Banglore, India.
19. Mallik, A. K., Kher, V., Puri, M., and Hatwal, H., "On the Modelling of Non-linear Elastomeric Vibration Isolators," *Journal of Sound and vibration*, Vol. 219, 1999, pp. 239-253.
20. Jordon, D. W., and Smith, P., *Nonlinear Ordinary Differential Equations*, Clarendon Press, Oxford, England, U.K., 1977.